

Article

An Experimental Study on Progressive and Reverse Fluxes of Sediments with Fine Fractions in the Wave Motion over Sloped Bed

Iwona Radosz ^{1,*}, Jerzy Zawisza ¹, Jarosław Biegowski ², Maciej Paprota ², Dawid Majewski ²
and Leszek M. Kaczmarek ¹

¹ Faculty of Civil Engineering, Environmental and Geodetic Sciences, Koszalin University of Technology, Sniadeckich 2, 75-453 Koszalin, Poland

² Institute of Hydro-Engineering, Polish Academy of Sciences, Kościarska 7, 80-328 Gdansk, Poland

* Correspondence: iwona.radosz@tu.koszalin.pl

Abstract: The purpose of the study was to collect experimental data on the vertical structure of sediment fluxes during the wave crest and trough phase over sloped bed. The first stage of the experimental work included measurements of these fluxes using the particle image method, while the second stage, measurements of sediment transport rates and granulometric distributions of sediments collected in the traps on both sides of the sloped initial area. The experimental data were compared both with the results collected previously over flat bed as well as with a theoretical analysis based on a three-layer model of graded sediment transport. This model does not take into account the effects related to the presence of fine and very fine fractions and neglects the effects related to the bed slope, i.e., to gravitational forces and to additional pressure gradients. Hence, a modification of this model is proposed that is based on four coefficients that corrected for sediment fluxes over sloped bed. The consistency of the sediment transport calculations according to the modified model with measurements was achieved within plus/minus a factor of 2 of the measurements.

Keywords: sediment fluxes; wave crest; wave trough; sloped bed; sediment transport; grain size distributions; fine sediment fractions; particle image velocimetry (PIV) method



Citation: Radosz, I.; Zawisza, J.; Biegowski, J.; Paprota, M.; Majewski, D.; Kaczmarek, L.M. An Experimental Study on Progressive and Reverse Fluxes of Sediments with Fine Fractions in the Wave Motion over Sloped Bed. *Water* **2023**, *15*, 125. <https://doi.org/10.3390/w15010125>

Academic Editor: Maria Mimikou

Received: 8 November 2022

Revised: 11 December 2022

Accepted: 14 December 2022

Published: 29 December 2022

Corrected: 10 May 2023



Copyright: © 2022 by the authors. Licensee MDPI, Basel, Switzerland. This article is an open access article distributed under the terms and conditions of the Creative Commons Attribution (CC BY) license (<https://creativecommons.org/licenses/by/4.0/>).

1. Introduction

The problems of sediment transport in wave motion and the associated morphological changes of the bed are important from the point of view of engineering practice. Issues related to sediment transport include coastal erosion, sanding of waterways, design and operation of hydraulic constructions. Modeling the intensity of sediment transport in wave motion is an important but also challenging subject in coastal engineering, as sediment is transported intensively mainly in a very thin layer with a high concentration just above the bed. A number of previous studies, e.g., Wilson [1] and Sumer et al. [2], suggest that the thickness of such a layer depends on the sediment diameter and Shields' parameter and may range from only a few mm to a few cm. Consequently, the movement of water-soil mixture causes intensive segregation of sediment grains near the bed, with the process of most intensive sediment sorting occurring in the zone directly above the bed where grains are pulled up from the bed and collide with each other.

In the history of mathematical modeling development of sediment transport, there have been a huge number of studies devoted to the mechanisms of granulometrically homogeneous sediment movement and a significantly smaller number of studies on the transport of granulometrically heterogeneous sediment, i.e., being a mixture of multiple fractions with different d_i diameters. This is most likely due to the complexity of physical processes involved in transport, which is difficult to describe using simple empirical formulas that prevailed at a time when computer calculations were not possible. With the development

of computer technology and numerical methods, as well as the growing importance of hydraulic engineering, attempts have been made to develop theoretical descriptions that allow the prediction of granulometrically heterogeneous sediment transport.

Theoretical papers on the movement of granulometrically heterogeneous sediments with a description that takes into account both transported and suspended sediment has been summarized by Samaga et al. [3] and Karim [4]. Most of the successively appearing papers take into account the interaction of sediment fractions through the use of the so-called hiding and exposure parameter. The authors used these parameter as coefficients to reduce critical stresses for specific sediment fractions, depending on the content of other fractions. Wu et al. [5] described this parameter using a probability density function. Probability theory in describing the transport of granulometrically heterogeneous sediments has also been used by many other authors, such as Blom et al. [6].

In 2021, Khosravi K. et al. [7] attempted to determine hydraulic parameters under initial movement conditions for homogeneous and heterogeneous sediments, and Sun et al. [8] developed a description of the vertical distribution of heterogeneous sediment in suspension. This model allows the prediction of vertical granulometric variability, using separate characteristics for each sediment fraction, such as the values of the critical friction parameter, diameters and settling velocities. However, an independent reference concentration value is required for each fraction, at some distance from the bed. This makes the model relatively difficult to use in practice.

Over the years, several papers have been also devoted to sediment segregation under oscillatory motion. Ribberink [9] described the transport of each of the specified sediment fractions as a function of dimensionless friction. Dohmen-Janssen [10] introduced an amendment to Ribberink's [9] heterogeneous sediment transport formula to account for the effect of phase shift between the concentration of suspended sediment and the instantaneous velocity of water. In this simplified way, bidirectional sediment transport under wave conditions is described, with coarser fractions moving toward the shore and finer fractions moving in the opposite direction. In contrast, Hassan [11] proposed description of the bidirectional transport of granulometrically heterogeneous sediments under wave conditions using Bailard's quasi-stationary model [12].

The papers described above were dedicated to flow conditions with small or moderate bed gradients. The effect of steeper bed gradients on the intensity of sediment transport is quite obvious and intuitive, and therefore it was natural for many authors to focus on this topic in order to develop an adequate description. Shields [13], in his paper, on the basis of conducted measurements, noted that for equal grain diameters, the intensity of sediment transport increases along with increasing bed slope. Due to the fact that most of the classical formulae for sediment transport are functions of the critical Shields parameter, many authors naturally directed their investigations to seek for a corrected value of this parameter under conditions of laboratory measurements at significant bed slopes. The authors [14–17] mostly attempted to modify the Meyer-Peter and Müller formula [18]. Lamb et al. [19] presented a one-dimensional mathematical model derived under the assumption of vertical equilibrium of forces acting on the sediment, using a classical description of turbulence with a mixing path. Recking [20] proposed describing the critical Shields stress as a function of bed slope, grain diameter, dynamic velocity, internal friction and resistance coefficient. In his paper, he pointed out the increasing trend in the value of critical Shields parameter as the slope increases. Parker et al. [21] corrected the values of Shields parameter for large gradients based on 3 series of laboratory measurements by other authors. Maurin et al. [22] also presented a description of sediment transport for large bed gradients that is a function of the modified Shields critical stress value. However, researchers summarizing their study noted that the bed slope may not affect only the value of this parameter, but a number of physical processes accompanying sediment transport.

King [23], in his study in Oscillating Water Tunnel (OWT), measured the average value of sediment transport during the half-period of sinusoidal flow on a sloping bed. His experimental results showed that the bed slope influences the value of half-period

transport depending on the direction and inclination of a bed slope. Therefore, changes in the resultant transport rate during the wave period can be expected.

Tan W. and Yuan J. [24,25] described an experimental study in which resultant sediment transport during the wave period was measured in OWT, under sinusoidal oscillatory flows over a sloping bed. On the basis of their measurements, they argued that the effects induced by the bed slope on resultant sediment transport during the wave period may be as important as effects due to the slope or asymmetry of the wave. The same team [26] presented a two-layer model of sediment transport in wave motion, taking into account the effect of phase lags.

It is worth noting, however, the importance of statistical uncertainty in collecting experimental data of the main hydrodynamic features in the laboratory-scale measurements [27,28]. So, advanced statistical and stochastic analysis are welcome in the management and monitoring of natural resources [29,30].

The main aim of the present study was to collect experimental data documenting the vertical structure of sediment fluxes outgoing in both directions from the computational area to adjacent control areas (and retained in traps), as well as the granulometric composition of these sediments on both sides of the output area under sloping bed conditions. Knowledge of these quantities allows to expand our knowledge of sediment transport in the crest and trough phase of the wave over the sloping bed, respectively, and allows to compare the obtained results with the measured results obtained over the flat bed [31]. The experimental results were then confronted with the results of theoretical analysis based on the three-layer model of heterogeneous sediment transport [32].

The achievement of this goal was carried out experimentally in two stages. The first one involved experimental identification of suspended sediment fluxes using the PIV method. The second experimental stage involved measurements of fluxes retained in traps along with determination of the granulometric composition of transported sediments. Due to the fact that the theoretical model neglects the effect of vertical sorting of sediments with the content of i -th very fine fractions in the diameter range of $d_i < 0.20$ mm, and does not take into account the effects related to the bed slope, such as the effect of gravitational forces on sediment grains and the additional effect of reduced or increased pressure when changing the flow cross-section, it was proposed to modify the theoretical model with the above-mentioned effects.

Theoretical foundations of sediment transport modeling were formulated by Kaczmarek [33], who presented the concept of a multilayer continuous description of sediment concentration and velocity distributions. This concept was later extended by Kaczmarek and Ostrowski [34] to describe the transport of homogeneous sediments under wave-current conditions and by Kaczmarek et al. [35] to describe the transport of granulometrically heterogeneous sediments under wave-current conditions, as well as by Kaczmarek et al. [36,37] to describe morphological changes. The theoretical basis on the multilayer model of transport of granulometrically heterogeneous sediments under both wave and flow conditions is summarized by Kaczmarek et al. [32,38,39]. The presented theoretical model verified by present experiments is, on the one hand, a continuation of the latest achievements in the area of research on the wave transport [7,8,24–30], but at the same time proposes a “new way” of research, focusing not on the resultant transport in time, but on the separately considered transport in the crest and trough of the wave.

2. Materials and Methods

2.1. Theoretical Investigations

2.1.1. Description of the Flow

This paper assumes that due to the different nature of physical processes occurring at different distances from the bed, it is necessary to use different assumptions and equations to describe the vertical structure of sediment transport. The basic multilayer model [32,35] presents three main layers with separated sub-layers. The first layer of the model is characterized by a very high concentration of sediment in the immediate vicinity, i.e., directly above and below the conventional bed line, in which drag movement dominates.

The second layer—the contact layer—is also characterized by a high concentration but lower enough that vertical sorting of grains is possible. The third layer is an area of well-sorted suspended sediment, with very low concentration [31].

It is assumed [32,35] that in a moving layer of densely compacted sediments, all sediment fractions, at each level from the bed, move at a velocity equal to the velocity of the mixture at that level, and the interactions between sediment fractions are so strong that finer fractions are slowed down by coarser ones. The model also takes into account that the most intense vertical sorting of sediment occurs in the contact layer, where turbulent fluid pulsations and chaotic grain collisions cause the magnitudes of instantaneous velocities $u(z,t)$ and concentrations $c(z,t)$ to differ for individual fractions.

Theoretical model does not take into account the effect of phase lags on sediment transport, which is dictated by the assumption of an instantaneous bed response to friction that varies during the wave period, as well as the effects of vertical sorting of very fine fractions, which results in these fractions being lifted high above the bed and simultaneous bed loss.

When considering the components of sediment transport involving fine and very fine fractions over a sloping bed, due to the varying nature of the physical processes occurring at different distances from the bed, several layers can be distinguished to facilitate the description of vertical structure of sediment transport flowing out of the control area. Figure 1 after [31] schematically depicts the vertical structure of sediment transport in wave motion over a sloping bed, divided into the crest and trough phases of the wave. The positive direction of sediment transport is described according to the wave direction (Figure 1). The vertical transport structure includes suspended sediment fluxes $q_{f1}^{+/-}$, $q_{f2}^{+/-}$ and $q_{f3}^{+/-}$, as well as fluxes of sediment feeding traps, i.e., fluxes of $q_{st1}^{+/-}$ i $q_{st2}^{+/-}$. The fluxes $q_{f1}^{+/-}$ are the result of phase lags between water and fine fractions in the range of $d_i < 0.20$ mm, while fluxes $q_{f2}^{+/-}$ and $q_{f3}^{+/-}$ are the result of vertical sorting of granulometrically heterogeneous sediment, resulting in very fine fractions being lifted very high above the bed. It is worth recalling that the return fluxes of suspended sediments $q_{f1}^{+/-}$, $q_{f2}^{+/-}$ and $q_{f3}^{+/-}$ mix with each other and form a depth-averaged flux during the return phase:

$$\langle \varphi^{+/-}(z) \rangle = \frac{q_{f1}^{+/-} + q_{f2}^{+/-} + q_{f3}^{+/-}}{(\delta - \delta'_m)}, \quad (1)$$

In addition, theoretical model does not take into account the direct effect of bed slope on sediment transport. One such influence is the effect caused by gravitational forces acting on all grains, but most obviously on coarse grain fractions ($d_i \geq 0.2$ mm). Another effect related to the bed slope is that caused by pressure gradients. It consists in the formation of areas with reduced or increased pressure occurring at varying flow cross sections. In fact, when the movement of sediment over a sloping bed is considered, it is possible to see a decrease in the flow cross-section and a decrease in depth in the wave direction. Consequently, as the cross-section decreases in the crest phase, velocities increase and pressure decreases, and a negative pressure gradient is created. It is worth noting that sediment flow increases because the frictional forces that cause it increase with the additional forces from the negative pressure gradient. In the trough, the situation is reversed—frictional forces causing sediment movement are reduced by forces from a positive pressure gradient. When the cross-section increases and the pressure increases and a positive pressure gradient is generated then the velocities decrease and, as a result, the intensity of sediment transport also decreases. Therefore, it can be expected that the outgoing sediment flows toward the trap in the wave trough phase, as well as the returning flows, will be smaller than the flows in the flat bed situation. Especially in the zone near the bed, mainly coarse grains will be retained and will fall directly into the trap, while the return flux q_{f3}^- will feed the flux q_{st}^- . It is expected that the above effect, will have less impact on the fluxes of suspended grains $q_{f1}^{+/-}$ and $q_{f2}^{+/-}$, but always the return fluxes will be smaller than the fluxes for a flat bed due to the smaller hydrodynamic forcing. In

the wave crest phase, the situation is reversed. In this phase, it is expected that due to greater hydrodynamic forcing, the fluxes entering the trap will be larger than in the flat bed situation, which means that the return flow q_{f3}^+ will also feed the flux q_{st}^+ . However, at the same time, the return fluxes will decrease, as more of the total flux leaving the control area will feed the trap, but still they are greater than the fluxes for a flat bed due to the greater hydrodynamic forcing.

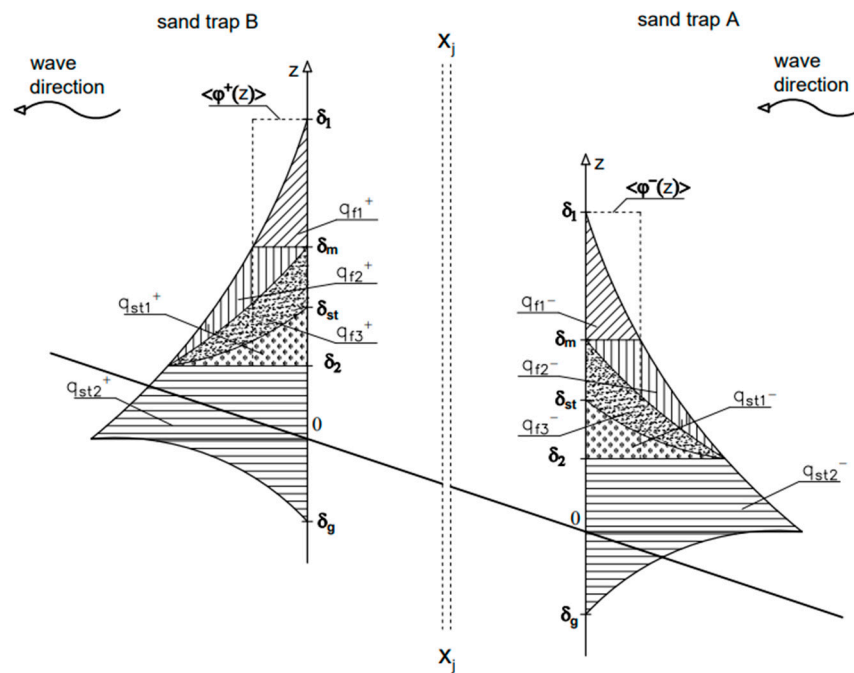


Figure 1. Vertical structure of the wave-induced progressive and reverse sediment fluxes over sloped bed.

2.1.2. Sediment Transport during the Wave Crest and Trough Phase

Theoretical analysis is proposed to be based on the three-layer heterogeneous sediment model of Kaczmarek et al. 2022 [32]. However, this model does not take into account the effects of additional vertical sorting of very fine sediment fractions and neglects the effects of phase lags of fine fractions, as well as does not take into account the effects related to the bed slope, i.e., effect of gravitational forces acting on grains, and the effect of pressure gradients when changing the flow cross section. Therefore, it is proposed to modify this model based on experimental results.

It is postulated to describe the theoretical fluxes $(q_{st}^{+/-})_{calc.}$ (calculated by the Kaczmarek et al. 2022 model) as the sum of fluxes of fine and very fine fractions $(q_f^{+/-})_{calc.}$ with diameter $d_i < 0.20$ mm and coarse fractions $(q_c^{+/-})_{calc.}$ with diameter $d_i \geq 0.20$ mm, as follows:

$$(q_{st}^{+/-})_{calc.} = (q_f^{+/-})_{calc.} + (q_c^{+/-})_{calc.}, \tag{2}$$

where

$$(q_c^{+/-})_{calc.} = \sum_{i=1}^{N_f} n_{fi} (q_{fi}^{+/-})_{calc.}, \tag{3}$$

$$(q_c^{+/-})_{calc.} = \sum_{i=N_f}^N n_{ci} (q_{ci}^{+/-})_{calc.}, \tag{4}$$

where:

- n_{fi} —proportion of the i -th fine and very fine fraction ($d_i < 0.2$ mm) in the input mixture;
- n_{ci} —proportion of the i -th coarse fraction ($d_i \geq 0.2$ mm) in the input mixture;

$(q_{fi}^{+/-})_{calc.}$ —transport rate of the i -th fine and very fine fraction ($d_i < 0.2$ mm), calculated using the Kaczmarek et al. 2022 model;

$(q_{ci}^{+/-})_{calc.}$ —transport rate of the i -th coarse fraction ($d_i \geq 0.2$ mm), calculated using the Kaczmarek et al. 2022 model;

$i = N_f$ —fraction with a diameter of $d_i = 0.2$ mm.

Modification of the flux calculation results (2) was proposed based on the correction factors $\beta_1^{+/-}$ and $\beta_2^{+/-}$ determined from flux measurements $(q_{st}^{+/-})_{meas.}$ as follows:

$$q_{st}^+ = \beta_1^+ (q_f^+)_{calc.} + \beta_2^+ (q_c^+)_{calc.} \tag{5}$$

$$q_{st}^- = (q_f^-)_{calc.} + (q_c^-)_{calc.} + \beta_1^- (q_f^+)_{calc.} + \beta_2^- (q_c^+)_{calc.} \tag{6}$$

postulating the equality of fluxes $q_{st}^{+/-} = (q_{st}^{+/-})_{meas.}$, where:

$$(q_{st}^{+/-})_{meas.} = \sum_{i=1}^{N_f} (n_{fi}^{+/-})_{meas.} (q_{st}^{+/-})_{meas.} + \sum_{i=N_f}^N (n_{ci}^{+/-})_{meas.} (q_{st}^{+/-})_{meas.} \tag{7}$$

where:

$(n_{fi}^{+/-})_{meas.}$ —measured proportion of the i -th fine and very fine fraction ($d_i < 0.2$ mm) in the mixture collected from the trap;

$(n_{ci}^{+/-})_{meas.}$ —measured proportion of the i -th coarse fraction ($d_i \geq 0.2$ mm) in the mixture collected from the trap.

The values of correction factors can be found using relations (5)–(7) as follows:

$$\beta_1^+ = \frac{(q_{st}^+)_{meas.} \sum_{i=1}^{N_f} (n_{fi}^+)_{meas.}}{\sum_{i=1}^{N_f} n_{fi} (q_{fi}^+)_{calc.}} \tag{8}$$

$$\beta_2^+ = \frac{(q_{st}^+)_{meas.} \sum_{i=N_f}^N (n_{ci}^+)_{meas.}}{\sum_{i=N_f}^N n_{ci} (q_{ci}^+)_{calc.}} \tag{9}$$

$$\beta_1^- = \frac{(q_{st}^-)_{meas.} \sum_{i=1}^{N_f} (n_{fi}^-)_{meas.} - \sum_{i=1}^{N_f} n_{fi} (q_{fi}^-)_{calc.}}{\sum_{i=1}^{N_f} n_{fi} (q_{fi}^+)_{calc.}} \tag{10}$$

$$\beta_2^- = \frac{(q_{st}^-)_{meas.} \sum_{i=N_f}^N (n_{ci}^-)_{meas.} - \sum_{i=N_f}^N n_{ci} (q_{ci}^-)_{calc.}}{\sum_{i=N_f}^N n_{ci} (q_{ci}^+)_{calc.}} \tag{11}$$

2.1.3. Grain Size Distributions of Transported Sediments

During wave motion in the crest and trough phases over a sloping bed, there are obvious changes in the granulometric composition of transported sediment with the proportion of fine and very fine fractions. The proportion of fine and coarse fractions transported during wave motion over a sloping bed can be described by the sum of the i -th fractions, distinguishing between fine fractions ($d_i < 0.2$ mm) and coarse fractions ($d_i \geq 0.2$ mm):

$$(n_f^{+/-})_{meas.} = \sum_{i=1}^{N_f} (n_{fi}^{+/-})_{meas.} \tag{12}$$

$$(n_c^{+/-})_{meas.} = \sum_{i=N_f}^N (n_{ci}^{+/-})_{meas.} \tag{13}$$

The proportion of fine and very fine $(n_f^{+/-})_{calc.}$ and coarse $(n_c^{+/-})_{calc.}$ fractions in the trap, as calculated using the model of Kaczmarek et al. 2022, can be described as follows:

$$(n_f^{+/-})_{calc.} = \frac{\sum_{i=1}^{N_f} n_{fi} (q_{fi}^{+/-})_{calc.}}{\sum_{i=1}^{N_f} n_{fi} (q_{fi}^{+/-})_{calc.} + \sum_{i=N_f}^N n_{ci} (q_{ci}^{+/-})_{calc.}}, \tag{14}$$

$$(n_c^{+/-})_{calc.} = \frac{\sum_{i=N_f}^N n_{ci} (q_{ci}^{+/-})_{calc.}}{\sum_{i=1}^{N_f} n_{fi} (q_{fi}^{+/-})_{calc.} + \sum_{i=N_f}^N n_{ci} (q_{ci}^{+/-})_{calc.}}, \tag{15}$$

To calculate the proportion of fine and very fine ($d_i < 0.2$ mm) and coarse ($d_i < 0.2$ mm) fractions for any given granulometric distribution of non-cohesive sediments with the proportion of very fine and fine fractions over a sloping bed, it is proposed to use correction factors described by relations (8)–(11). Then the proportion of fine and very fine fractions $(n_f^+)_{st}$ and coarse fractions $(n_c^+)_{st}$ caught in the trap in the crest phase over the sloping bed can be calculated as the transport ratio of fine/coarse fractions to the total transport in the crest phase, according to the following formulas:

$$(n_f^+)_{st} = \frac{\beta_1^+ \sum_{i=1}^{N_f} n_{fi} (q_{fi}^+)_{calc.}}{\beta_1^+ \sum_{i=1}^{N_f} n_{fi} (q_{fi}^+)_{calc.} + \beta_2^+ \sum_{i=N_f}^N n_{ci} (q_{ci}^+)_{calc.}}, \tag{16}$$

$$(n_c^+)_{st} = \frac{\beta_2^+ \sum_{i=N_f}^N n_{ci} (q_{ci}^+)_{calc.}}{\beta_1^+ \sum_{i=1}^{N_f} n_{fi} (q_{fi}^+)_{calc.} + \beta_2^+ \sum_{i=N_f}^N n_{ci} (q_{ci}^+)_{calc.}}. \tag{17}$$

In the trough phase, the magnitude $(n_f^-)_{st}$ and $(n_c^-)_{st}$ can be described as follows:

$$(n_f^-)_{st} = \frac{\sum_{i=1}^{N_f} n_{fi} (q_{fi}^-)_{calc.} + \beta_1^- \sum_{i=1}^{N_f} n_{fi} (q_{fi}^+)_{calc.}}{\sum_{i=1}^{N_f} n_{fi} (q_{fi}^-)_{calc.} + \sum_{i=N_f}^N n_{ci} (q_{ci}^-)_{calc.} + \beta_1^- \sum_{i=1}^{N_f} n_{fi} (q_{fi}^+)_{calc.} + \beta_2^- \sum_{i=N_f}^N n_{ci} (q_{ci}^+)_{calc.}}, \tag{18}$$

$$(n_c^-)_{st} = \frac{\sum_{i=N_f}^N n_{ci} (q_{ci}^-)_{calc.} + \beta_2^- \sum_{i=N_f}^N n_{ci} (q_{ci}^+)_{calc.}}{\sum_{i=1}^{N_f} n_{fi} (q_{fi}^-)_{calc.} + \sum_{i=N_f}^N n_{ci} (q_{ci}^-)_{calc.} + \beta_1^- \sum_{i=1}^{N_f} n_{fi} (q_{fi}^+)_{calc.} + \beta_2^- \sum_{i=N_f}^N n_{ci} (q_{ci}^+)_{calc.}}. \tag{19}$$

2.2. Experimental Investigations

2.2.1. Experimental Set-Up

Experimental objectives were achieved in the wave-current channel at the hydraulic laboratory of the Institute of Hydro-Engineering Polish Academy of Sciences in Gdańsk in 2021. The channel is equipped with measuring and supporting equipment necessary for the research. The wave tank with glass walls is 64 m long and 0.6 m wide. Operational water depths typically range from 0.2 m to 0.8 m. The channel is equipped with vertical glass walls, parallel to each other, that allow unobstructed observation of the research being carried out and the use of PIV (Particle Image Velocimetry) imaging anemometry techniques. Waves are generated by a piston-type generator installed at the upstream end of the flume. The currently described experiments with a sand bed were carried out in a separate section of the trough, as shown in Figure 2. The section was bounded with a wave absorber to eliminate the effect of wave reflection. Installation of the trap structure in the sandy bed required modifications to the original geometry of the flume. The original bed was modified to achieve a bed angle of 15°, and then traps were inserted between the new sloping bed structure. Tests were conducted for a water level corresponding to a upstream depth of $h = 0.50$ m.

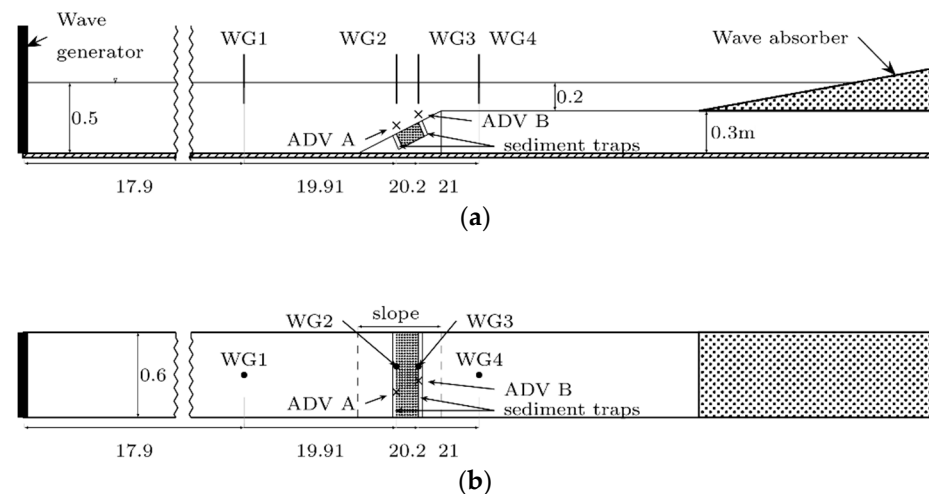


Figure 2. Experimental setup in a wave flume for measurements of wave-induced sediment transport on a sloping bed: (a) side view of the wave flume with the sand box implemented; (b) top view of the wave flume with position of gauges and sand traps.

Twelve tests were conducted to measure the amount of sediment transport over a sloping bed. During all experiments, simultaneous sampling of sediments trapped in traps on both sides of a control area was carried out. A set of resistance probes recording data at a sampling rate of 100 Hz was used to measure changes in the elevation of free water surface. Measurements of the velocity of water particles were conducted using ADV (Acoustic Doppler Velocimeter) ultrasonic velocimeters recording at 25 Hz. A system of wave gauges (WG) of the resistive type was used to measure the height and periodicity of changes in free surface of water.

A proprietary structure consisting of a main “tray” (sand section) and “traps” (sediment traps) was used to carry out measurements to determine the amount of transport of non-cohesive and granulometrically heterogeneous sediments with an arbitrary granulometric distribution. This structure was made of a waterproof plywood and plastic panels, painted all black, installed in front of and behind the sand section. The structure consisted of two traps A and B, of size $100 \times 560 \times 100$ mm, and a box/tray located between traps, of size $300 \times 560 \times 100$ mm.

Measurement tests were carried out for 4-four sediments, without changing the wave conditions, i.e., wave height, wave period, as well as the experiment duration. Using computer software controlling the wavemaker, a regular wave was generated. Wave parameters were recorded using four wave probes distributed along the length of the flume, i.e., two in front of and two behind the tray structure. Table 1 shows the basic experimental parameters.

Table 1. Basic data of the flat bottom experiment—IBW PAN 2021.

Parameter	Symbol	Value	Unit
Water depth	h_0	0.50	m
Wave height	H_w	0.12	m
Test duration	T_w	10	min
Wave peak period	T_p	3.0	s
Representative diameter of bottom-building sediment grains	d_{50}	A: 0.38 B: 0.32 C: 0.25 D: 0.14	mm
Sediment density	ρ_s	2.62	g/cm^3
Liquid density	ρ_w	1.00	g/cm^3
Sediment porosity	n_p	0.4	–

2.2.2. Scope of the Measurement

Four types of quartz sands with granulometric characteristics summarized in Table 2 were selected for the experiments.

Table 2. Granulometric characteristics of the studied sands.

Type of Sand	$d_{90}/d_{50}/d_{10}$
A. Coarse quartz sand	0.58/0.38/0.24
B. Medium quartz sand	0.48/0.32/0.20
C. Fine quartz sand	0.38/0.25/0.16
D. Very fine quartz sand	0.19/0.14/0.08

The sands were subjected to granulometric analysis. For this purpose, a MikroLAB sieve shaker, model LPzE-2e, was used. Measurements were made using the “dry” method, for all collected sediment samples. Prior to testing, samples were taken from a container filled with sediment prepared for testing, while after each test, a sample was taken from traps A and B. Samples taken from traps were dried at 100 °C for 24 h before granulometric analysis. For all the measurements carried out, essentially the identity of results was obtained. The cumulative grain size curves of the four sediments are shown in Figure 3.

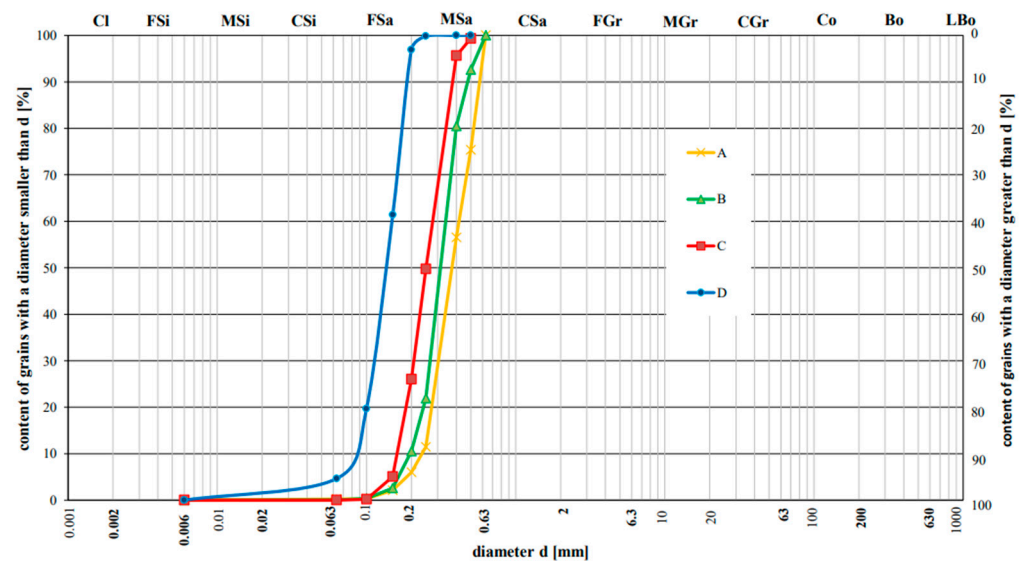


Figure 3. Grain size distribution of quartz sands used in the experiment A: $d_{50} = 0.38$; B: $d_{50} = 0.32$; C: $d_{50} = 0.25$; D: $d_{50} = 0.14$.

As can be seen from the grain size curves prepared, the analyzed sandy sediments can be divided into two types:

- sandy with a very high proportion of fine fractions ($d_{50} < 0.20$ mm; sand D: grain content $d_i < 0.20$ mm = 97%);
- sandy with low content of fine fractions ($d_{50} \geq 0.20$ mm; grain content $d_i < 0.20$ mm equal to sand A: = 6%, B: = 10.5%, C: = 26%, respectively).

Each measurement test was carried out according to the following procedure. Waves with preset characteristics were generated for 10 min (Table 1). After that, the measurements of the bathymetry of bed in the center of control area and the mass of sand in both settling tanks were conducted. A total of 12 measurement series were carried out covering 4 types of sand with 3 repetitions of each case. Bathymetric measurements were carried out using a bar with rods with flat weights attached to their end.

Sediment was transported to trap B during the wave crest, and to trap A during the trough of the wave. At the end of each wave projection, in order to determine the volume of accumulated sand in traps, the sediment had to be brought out into the channel. For this purpose, the siphoning method was used. With silicone hoses, the mixture of water and sediment was pumped out of the extreme boxes into two separate boxes. The samples were then transferred to flasks, which were filled with water to a known volume. The flasks with the sediment and water were weighed, and the weight and volume of sediment extracted from each trap was determined on this basis.

3. Results and Discussion

3.1. Free Stream Velocity Measurements

The gravity waves induce orbital velocity as they propagate. These velocities observed at the edge of the wave boundary layer are called the free stream velocities [40]. The velocities were estimated based on ADV records performed at the distance of 6 cm above the sand box edges as presented in Figure 2. The recorded horizontal (the X) component of particle velocity was divided in the time series covering one wave period. This set of curves was used to estimate the characteristic distribution of velocities during one wave period by taking the mean value in particular time. The resultant curve is denoted by blue line in Figure 4. The next step of the procedure involved the decomposition of the mean value into the Fourier series. The estimated Fourier coefficients were used to reproduce the mean velocity with $n = 4$ harmonics according to the Equation (20). The coefficients are summarized in Table 3. Moreover, the Fourier series coefficients provided the analytical solution used as an input for numerical model.

$$f(t) = 0.5a_0 + \sum_{i=1}^{i=n} (a_n \cos(n2\pi t) + b_n \sin(n2\pi t)), \tag{20}$$

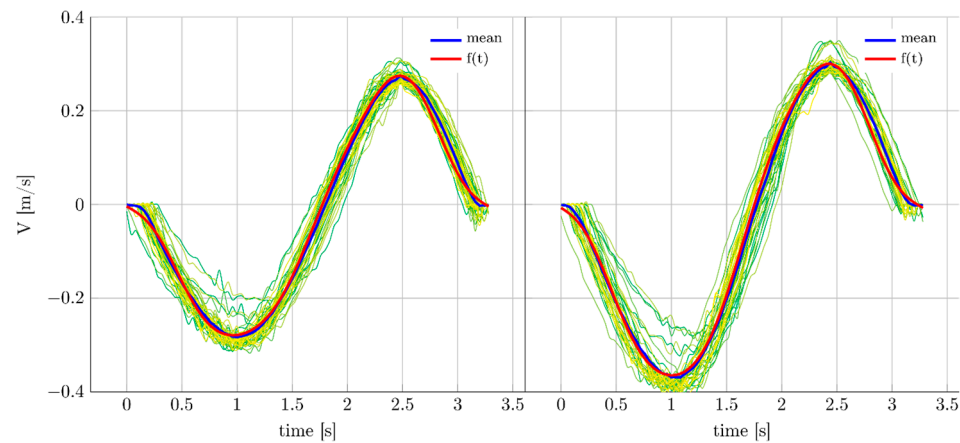


Figure 4. Characteristic records of the along flume particle velocities recorded by ADV A (left) and ADV B (right).

Table 3. Summary of Fourier series coefficients used as an input to numerical model for wave parameters: $T = 3.0$, $Hw = 0.12$.

$0.5 \cdot a_0$	a1	b1	a2	b2	a3	b3	a4	b4	ADV
-0.0216	0.0389	-0.2504	-0.0216	0.0358	-0.0022	0.0216	0.0025	0.0107	A
-0.0395	0.0396	-0.3023	-0.0121	0.0611	0.0003	0.0198	0.0045	0.0116	B

As a result of this procedure the curve $f(t)$ was obtained and is denoted by red line in Figure 4. The horizontal velocities recorded on the sloping bottom are compared in Figure 5 and are fairly symmetrical. Especially velocities recorded by ADV A which was installed

lower on the slope, i.e., deeper. Moreover the velocities measured by the downstream gauge (ADV B—color blue) are higher in magnitude due to the wave shortening as it shoals. Velocities recorded by the this ADV kept their horizontal asymmetry low but vertical asymmetry for these velocities increased resulting in higher velocities directed against the wave propagation. This increase in maximal velocity in the direction opposite to the wave was also noted by Elfrink et al. [41] and it affects the vertical asymmetry of orbital velocity. This is confirmed by the comparison of the difference of maximal and minimal acceleration for that case. The offshore direction of the period averaged near bottom horizontal velocity influence the cross shore sediment transport. Zou et al. [42] in their studies noticed that the sloping bottom has a significant effect on vertical orbital velocities but not on horizontal velocities and shear stress. Moreover, the asymmetry of the considered velocities is much lower than the corresponding values recorded for flat bottom [31].

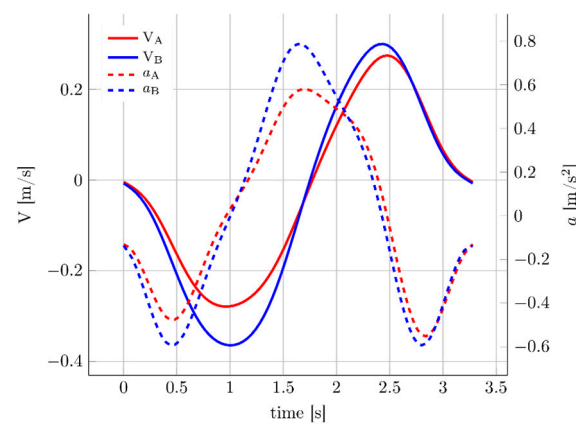


Figure 5. Characteristic records of horizontal particle velocities recorded by ADV A (left) and ADV B (right).

In addition, the increase in maximum velocity in the trough of wave propagating over the sloping bed means that the radical decrease in frictional forces causing sediment movement, forced by the forces of positive pressure gradient, is inhibited.

3.2. PIV Measurements

Using the methodology based on PIV and extensively described in [31], phase-averaged sediment fluxes for the sloping bottom case were calculated according the formulas:

$$q_{\frac{A}{B}} = \frac{1}{\delta} \int_0^{\delta} u(x_{\frac{A}{B}}, z, t) dz, \tag{21}$$

where $\delta = 0.5$ and 2 cm, while $x_A = -0.16$ m and $x_B = 0.16$ m. The instantaneous fluxes expressed by (21) were conditionally averaged over one wave period for consecutive waves. This conditional average refers to the negative (opposing the wave) and positive (following the wave) fluxes through the given cross section, which may be expressed as:

$$\hat{q}_{\frac{A}{B}}^+ = \frac{1}{T} \int_0^T q_{\frac{A}{B}} dt, \quad q_{\frac{A}{B}} > 0, \tag{22}$$

$$\hat{q}_{\frac{A}{B}}^- = \frac{1}{T} \int_0^T q_{\frac{A}{B}} dt, \quad q_{\frac{A}{B}} < 0. \tag{23}$$

The results are presented in Table 4 together with estimates of fluxes for the flat bottom case for convenience of comparison. It is worth remembering that the results obtained by the PIV method should be interpreted rather qualitatively, due to the very strong variability of concentration at the bed.

Table 4. The comparison of the wave-average values of the phase-averaged fluxes $\hat{q}_{(A/B)}$ in the flat bed conditions with the results in the sloped bed conditions.

$\delta = 0.5 \text{ cm—Flat Bed}$				
Case	Trough $h = 0.36 \text{ cm}$		Crest $h = 0.28 \text{ cm}$	
	\hat{q}_A from Sand Trap	\hat{q}_A to Sand Trap	\hat{q}_B to Sand Trap	\hat{q}_B from Sand Trap
Sand A	0.00012 (8.6%)	−0.00020 (4.5%)	0.00014 (11.1%)	−0.00009 (6.8%)
Sand B	0.00018 (3.7%)	−0.00025 (5.6%)	0.00008 (21.2%)	−0.00009 (8.7%)
Sand C	0.00022 (5.2%)	−0.00025 (3.9%)	0.00006 (16.4%)	−0.00007 (5.3%)
$\delta = 2.0 \text{ cm—Flat Bed}$				
Case	Trough $h = 0.36 \text{ cm}$		Crest $h = 0.28 \text{ cm}$	
	\hat{q}_A from Sand Trap	\hat{q}_A to Sand Trap	\hat{q}_B to Sand Trap	\hat{q}_B from Sand Trap
Sand A	0.00067 (7.2%)	−0.00061 (7.0%)	0.00042 (17.0%)	−0.00049 (8.6%)
Sand B	0.00094 (2.5%)	−0.00091 (8.1%)	0.00024 (24.5%)	−0.00038 (11.4%)
Sand C	0.00105 (3.1%)	−0.00091 (5.2%)	0.00016 (12.6%)	−0.00035 (6.4%)
$\delta = 0.5 \text{ cm—Sloped Bed}$				
Case	Trough $h = 0.36 \text{ cm}$		Crest $h = 0.28 \text{ cm}$	
	\hat{q}_A from Sand Trap	\hat{q}_A to Sand Trap	\hat{q}_B to Sand Trap	\hat{q}_B from Sand Trap
Sand A	0.00004 (8.0%)	−0.00018 (5.9%)	0.00033 (4.0%)	−0.00017 (4.9%)
Sand B	0.00004 (7.7%)	−0.00021 (7.0%)	0.00039 (3.5%)	−0.00015 (8.4%)
Sand C	0.00004 (7.5%)	−0.00017 (8.3%)	0.00033 (4.2%)	−0.00015 (8.4%)
Sand D	0.00005 (6.3%)	−0.00015 (4.5%)	0.00010 (9.6%)	−0.00013 (5.5%)
$\delta = 2.0 \text{ cm—Sloped Bed}$				
Case	Trough $h = 0.36 \text{ cm}$		Crest $h = 0.28 \text{ cm}$	
	\hat{q}_A from Sand Trap	\hat{q}_A to Sand Trap	\hat{q}_B to Sand Trap	\hat{q}_B from Sand Trap
Sand A	0.00049 (7.5%)	−0.00044 (8.4%)	0.00075 (6.2%)	−0.00078 (4.3%)
Sand B	0.00068 (3.8%)	−0.00085 (8.7%)	0.00106 (5.2%)	−0.00098 (7.0%)
Sand C	0.00061 (4.2%)	−0.00076 (8.8%)	0.00107 (6.2%)	−0.00094 (7.0%)
Sand D	0.00037 (6.1%)	−0.00073 (5.3%)	0.00049 (8.3%)	−0.00085 (4.3%)

The following conclusions from Table 4 however, can be deduced:

1. As can be assumed, in the situation of a sloping bed, the flux \hat{q}_B inside the near-wall layer (thickness $\delta \approx 0.5 \text{ cm} \approx \delta_m$, where δ_m is the thickness of the boundary layer as determined by the Kaczmarek et al. 2022 model) from the computational area and directed to the trap (positive values) reaches values clearly greater than the absolute values of flux \hat{q}_B returning to the computational area (Table 4). This is understandable, as the effect of a negative pressure gradient becomes apparent, which causes an increase in hydrodynamic forcing and an increase in flux values \hat{q}_B . For a flat bed, in the lack of a negative pressure gradient, the magnitudes of fluxes leaving and returning to the computational area are much smaller. Under the conditions of a sloping bed, only in case of sand D, i.e., in the situation of presence of a very large number of fine fractions in the bed, the fluxes \hat{q}_B returning are larger than those leaving. This is because the large number of very fine fractions in the fluxes q_{f1}^+ , q_{f2}^+ and q_{f3}^+ means a larger (after they are mixed) and closer to the bed averaged by depth return fluxes \hat{q}_B , at the boundary of near-wall layer.

In case of sediments A, B, C, the returning fluxes \hat{q}_B high above the bed ($\delta \approx 2.0 \text{ cm}$) are balanced with the fluxes leaving the control area. Only in the case of sediment D, the returning fluxes \hat{q}_B are larger than the outgoing fluxes, as the proportion of suspended fine and very fine fractions in this flux is dominant. In case of a flat bed, the returning fluxes (Table 4) are slightly larger, while in the case of a sloping bed, the negative pressure gradient causes more material (including fluxes q_{f3}^+) falls into the trap. As a result, the return fluxes are slightly smaller.

In summary, it can be expected that higher hydrodynamic forcing caused by a negative pressure gradient will cause the fluxes measured over a sloping bed to be closer to those calculated by the Kaczmarek et al. model of fluxes $(q_{st}^+)_{calc.}$, than in the flat bed situation;

2. Under sloping bed conditions, the fluxes \hat{q}_A both outgoing and entering the trap (with a minus sign) in the wave trough phase are smaller than the fluxes \hat{q}_A under flat bed conditions. This is due to weaker hydrodynamic conditions caused by the effect of a positive pressure gradient, which reduces transport. In addition, at the bed the flux q_{f3}^- outgoing towards the trap in the area of positive pressure gradient additionally feeds the flux q_{st}^- . As a result, the fluxes entering traps will be significantly larger than those outgoing.

It is also worth noting, that in case of a sloping bed, the fluxes \hat{q}_A directed to traps (for sediments A, B, C) in the trough phase of the wave reach absolute values smaller than the fluxes \hat{q}_B in the crest phase of the wave (Table 4). The above observation seems to be understandable due to the effects occurring over the sloping bed, which increase fluxes \hat{q}_B and decreasing the fluxes \hat{q}_A . In turn, the fluxes \hat{q}_B outgoing from the trap (with a minus sign) are similar in value to the fluxes \hat{q}_A entering the trap on the opposite side (with a minus sign). This represents the opposite situation to that on a flat bed (Table 4), where fluxes \hat{q}_A entering the trap are clearly larger than the fluxes \hat{q}_B outgoing on the opposite side from the trap. Furthermore, taking into account the fact that under sloping bed conditions the flux in the trough phase \hat{q}_A directed to the trap is smaller than the flux \hat{q}_A under flat bed conditions, it can be expected that the effect of fine fractions in the trough of the wave on the acceleration of coarse fractions will be much smaller. On the other hand, the increased amount of material flowing into the trap (including very fine fractions) in the wave crest leads to expect that the effect of flushing very fine fractions from the bed occurring in the case of a flat bed will not take place in the situation of a sloping bed. Finally, it is worth noting that the effects caused by positive pressure gradient are so strong (Table 4) that even in areas higher up the bed ($\delta \approx 2.0 \text{ cm}$) for all types of sediments, the absolute values of flux \hat{q}_A from the calculation area and directed to the trap remain greater than the flux \hat{q}_A returning. This is because the latter is formed only by the fluxes q_{f1}^- and q_{f2}^- . This is the opposite situation from that on a flat bed, where the fluxes were balanced.

3.3. Correction Factors for Sediment Fluxes

The calculated correlation coefficients are shown in Figure 6a–d depending on Shields’ parameter $\theta_{2.5}$, i.e., dimensionless bed friction calculated by the Kaczmarek et al. 2022 model for the maximum tangential stress during the wave period. The coefficients were calculated using Formulas (8) ÷ (11) and then approximated by a correlation curve with a determination coefficient $R^2 \geq 0.80$. In order to obtain such a high fit value, a few results of calculated coefficients significantly deviating from the correlation curve were omitted. The deviations concerned cases of sand with a high content of very fine grains (type D; $d_{50} = 0.14$). In such cases, for the calculation of modified transport $q_{st}^{+/-}$ values were taken as arithmetic averages of the calculated quantities of $\beta_1^{+/-}$ i $\beta_2^{+/-}$ for all measurements of a given case. These quantities are marked with triangles in Figure 6a,b,c,d. Radical reduction of the coefficients $\beta_1^{+/-}$ (Figure 6a,c) for a bed composed of sediments with a large amount of fine and very fine fractions is due to the increase in fluxes $q_{f1}^{+/-}$, $q_{f2}^{+/-}$ and $q_{f3}^{+/-}$ at the expense of $q_{st}^{+/-}$. In addition, an increase in hydrodynamic impacts on the bed (increase in $\theta_{2.5}$) results in both an increase in fluxes $q_{f1}^{+/-}$, $q_{f2}^{+/-}$ and $q_{f3}^{+/-}$, as well as $q_{st}^{+/-}$, and this implies an increase in the coefficients $\beta_1^{+/-}$ with the increase of $\theta_{2.5}$. In turn, a dramatic increase in the coefficients $\beta_2^{+/-}$ for sand D implies an increased amount of fine and very fine fractions in the flow and their significant effect on increasing the proportion of coarse fractions in the transport (Figure 6b,d).

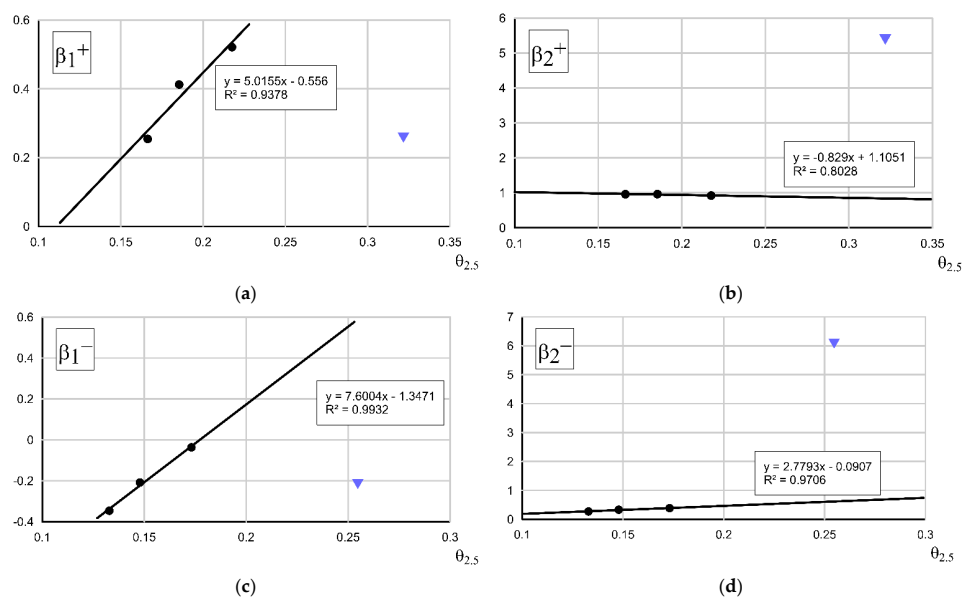


Figure 6. Plots of sediment flux correction factors over a sloping seabed: (a) fine fractions, crest phase; (b) coarse fractions, crest phase; (c) fine fractions, trough phase; (d) coarse fractions, trough phase.

It should be expected that under sloping bed conditions, in the zone of negative pressure gradient, the flux q_{f3}^+ will feed the flux q_{st}^+ to a much greater extent than in case of a flat bed. Only for sand D a larger amount of fine and very fine fractions feed the flux $q_{f1}^{+/-}$, $q_{f2}^{+/-}$, which returns to the initial area without filling traps. Therefore, it is not surprising that the values of β_1^+ coefficients for a sloping bed reach values greater than those of β_1^+ for the case of a flat bed (Table 5). The inverse relationship occurs only for sand D. However, in the zone of negative pressure gradient, it is expected, for all types of debris, including sand D, to increase (relative to the flat bed) the amounts of fine and very fine fractions and their effect on increasing the transport of coarse fractions. Hence, it can be expected that the values of β_2^+ coefficients, both under weak and stronger wave conditions, must increase relative to a flat bed, for all types of sands (Table 5). It is worth noting that the values of β_2^+ coefficients close to unity in the situation of a sloping bed (Figure 6b) indicate

a very good mapping of the measured transport values with the quantities calculated by the Kaczmarek et al. 2022 model.

Table 5. Comparison of the correction factors over a sloping and flat seabed in the wave crest phase and wave trough phase.

Crest				
Type of Sand	β_1^+ —Sloped Bed Case	β_1^+ —Flat Bed Case	β_2^+ —Sloped Bed Case	β_2^+ —Flat Bed Case
Sand A	0.278185	0.204274	0.96722	0.600155
Sand B	0.374075	0.308164	0.95137	0.759586
Sand C	0.535349	0.482891	0.924714	1.027727
Sand D	0.258206	1.049027	5.387826	1.896533
Trough				
Type of Sand	β_1^- —Sloped Bed Case	β_1^- —Flat Bed Case	β_2^- —Sloped Bed Case	β_2^- —Flat Bed Case
Sand A	−0.33714	−0.31215	0.278621	0.153719
Sand B	−0.22297	−0.12580	0.320369	0.531003
Sand C	−0.03117	0.187276	0.390508	1.164859
Sand D	−0.21587	1.199482	6.076916	3.214157

The behavior of coefficients for the fluxes in the trough phase of the wave can be described in a similar way, although the definition of β_1^- and β_2^- coefficients described by Formulas (10) and (11) differs from the definition of β_1^+ and β_2^+ described by Formulas (8) and (9). Under sloping bed conditions, in a zone of positive pressure gradient, a lower total flux is to be expected q^- outgoing from the control area. In addition, negative and less than unity values of β_1^- coefficients (Figure 6c) mean that the fluxes returning from the trough phase are reduced in magnitude q_{f3}^- mainly due to the increase q_{st1}^- at the expense of the latter flux. Thus, it is to be expected that the values of β_1^- coefficients will be smaller on a sloping bed, relative to a flat bed (Table 5). Of course, the lower flux of very fine and fine fractions, results in a smaller impact of these fractions on the transport of coarse fractions. The above statement does not apply to D-sand, where an increased amount of fine and very fine fractions returns, and as a result, they are expected to have a large effect on coarse fractions. The reduced influence of very fine fractions on coarse fractions, in the cases of sediments A, B, C, compared to the case of flat bed, makes one expect much smaller differences between the transport of coarse fractions estimated by the Kaczmarek et al. 2022 model and measured during the experiments. It is worth noting that the obtained values of $\beta_2^- = \beta_1^- \approx 0$ prove that the transport volumes in the wave trough q^- calculated with the Kaczmarek et al. 2022 model reproduce very well the quantities measured q_{st}^- under sloping bed conditions for sediment A, B and C. In case of sand D, it is expected that the calculated transport volumes of coarse fractions will be underestimated, while the calculated transport volumes of fine and very fine fractions will be overestimated. On the other hand, in the wave crest, under sloping bed conditions, due to the $\beta_2^+ = 1$ for A,B and C sand, the calculated volumes reflect the measured volumes very well. Again, for sediment D, increased differences are to be expected. Finally, it is worth noting that for sand A the β_2^- coefficient is larger for a sloping bed than for a flat bed. This situation occurs despite the fact that, in the case of a flat bed, there is a greater presence of fine and very fine fractions, increasing the transport of coarse fractions. From this, it shows the influence of gravity on the increase in transport of coarse fractions. Only in the presence of more fine and very fine fractions (sand B and C) above the flat bed is the effect of these fractions on the increase in transport of coarse fractions significantly greater than the effect of gravity. In case of sand D, the effects related to the influence of fine and very fine fractions on the transport of coarse fractions are dominant, particularly in the area of positive pressure gradient.

3.4. Comparison of Transport Calculations with Measurement Results

Comparison of the calculation results $(q_{st}^{+/-})_{calc.}$ carried out with the Kaczmarek et al. 2022 model according to Formulas (2)–(4) and the results of calculations $q_{st}^{+/-}$ carried out with the modified model according to Formulas (5) and (6) with the results of measurements $(q_{st}^{+/-})_{meas.}$ are shown from Figures 7–12. Letter (a) shows the results for a flat bed, and letter (b) shows the results for a sloping bed. The consistency discussion was carried out within $+/-$ a factor two of the measurements. Comparisons of calculation results with measurements were also carried out separately for the fluxes of fine and very fine fractions (Figure 7) and coarse fractions in the crest phase (Figure 8), as well as for the fluxes of fine and very fine fractions (Figure 10) and coarse fractions (Figure 11) in the trough phase. The results presented in Figures 7b, 8b, 9b, 10b, 11b and 12b suggest that very good agreement was obtained with the calculations of the Kaczmarek et al. 2022 transport model $(q_f^{+/-})_{calc.}$ and $(q_c^{+/-})_{calc.}$ as well as the modified model of Kaczmarek et al. 2022 $(q_f^{+/-})_{st}$ and $(q_c^{+/-})_{st}$ with the results of measurements over the sloping bed. This is as expected, given the positive and negative pressure gradient zones causing the measured fluxes to increase $q_{st}^{+/-}$.

The calculation results over a sloping bed $(q_{st}^+)_{calc.}$ do not differ significantly from the measurement results beyond the designated limits of agreement within $+/-$ a factor two of the measurements (Figure 9b). Larger differences can be observed only for sand D, composed mainly of fine and very fine fractions, which is related to the large amount of sediment returning in the trough phase to the initial area where it is retained. In addition, an underestimation of the calculated transport of coarse fractions in the crest can be observed for sand D $(q_c^+)_{calc.}$, due to the large amount of suspended fine and very fine fractions—increasing the measured transport of coarse fractions. Calculations of the intensity of sediment transport over a sloping bed in the wave trough $(q_{st}^-)_{calc.}$ (Figure 12b) also provide results that are consistent with the measurements within $+/-$ a factor two of the measurements. Only the coarse fractions in the flux are underestimated $(q_c^-)_{calc.}$ for sand D, which is due to the influence of very fine fractions on the transport of coarse fractions.

Finally, it is worth noting that over the flat bed the prediction by the Kaczmarek et al. 2022 model of fluxes in the crest phase $(q_{st}^+)_{calc.}$ (Figure 9a) mainly for weak hydrodynamic conditions ($h = 0.36$ m) and sediment D under stronger conditions ($h = 0.28$ m) provides values that are clearly overestimated compared to measured volumes. This is because the theoretical model does not take into account the return of fine and very fine fractions in the trough phase. This is particularly evident in the overestimation of calculated volumes $(q_f^+)_{calc.}$ (Figure 7a) in the wave crest and underestimation of calculated transport volumes $(q_{st}^-)_{calc.}$ (Figure 12a) and $(q_c^-)_{calc.}$ (Figure 11a) in the wave trough. It is worth noting that the prediction by the Kaczmarek et al. 2022 model of coarse fractions falling into the trap $(q_c^+)_{calc.}$ (Figure 8a) also gives overestimated results, as it does not take into account the loss from the bed and the suspension high above the bed of very fine fractions. As a result, the bed becomes rougher, reducing the measured transport values. This effect is offset in case of a sloping bed due to the zone of negative pressure gradient.

To sum up, in case of a flat bed composed of fine and very fine fractions, a large amount of material suspended above the bed and returning in the trough phase is formed in the crest, resulting in a reduced transport $q_{st}^{+/-}$ falling into the trap. In case of a sloping bed, due to the negative pressure gradient zone, a larger amount of transported sediment (both fine and coarse grains) in the wave crest falls into the trap. This results in better agreement between the results of calculations by the Kaczmarek et al. 2022 model and the measured results compared to the results from a flat bed. This agreement deteriorates in case of sediments with a high content of fine and very fine grains (sediment D), when the flux of coarse fractions falling into the trap is increased, while the flux of fine fractions falling into the trap is reduced, as most of the suspended material returns to the initial area. In the trough phase in case of a flat bed, the transport of returning finest fractions

is increased, which has the effect of increasing the transport of coarse fractions. This effect is weaker in case of a sloping bed, due to the positive pressure gradient zone. This is because the additional pressure gradient inhibits the increase in transport of both coarse and fine fractions, while increasing the sediment flow into the trap. This results in almost perfect agreement between calculations by the Kaczmarek et al. 2022 model and measurements. Again, only in case of sand D, the increased amount of very fine fractions in suspension results in an underestimation of the measured transport of coarse fractions by the Kaczmarek et al. 2022 model.

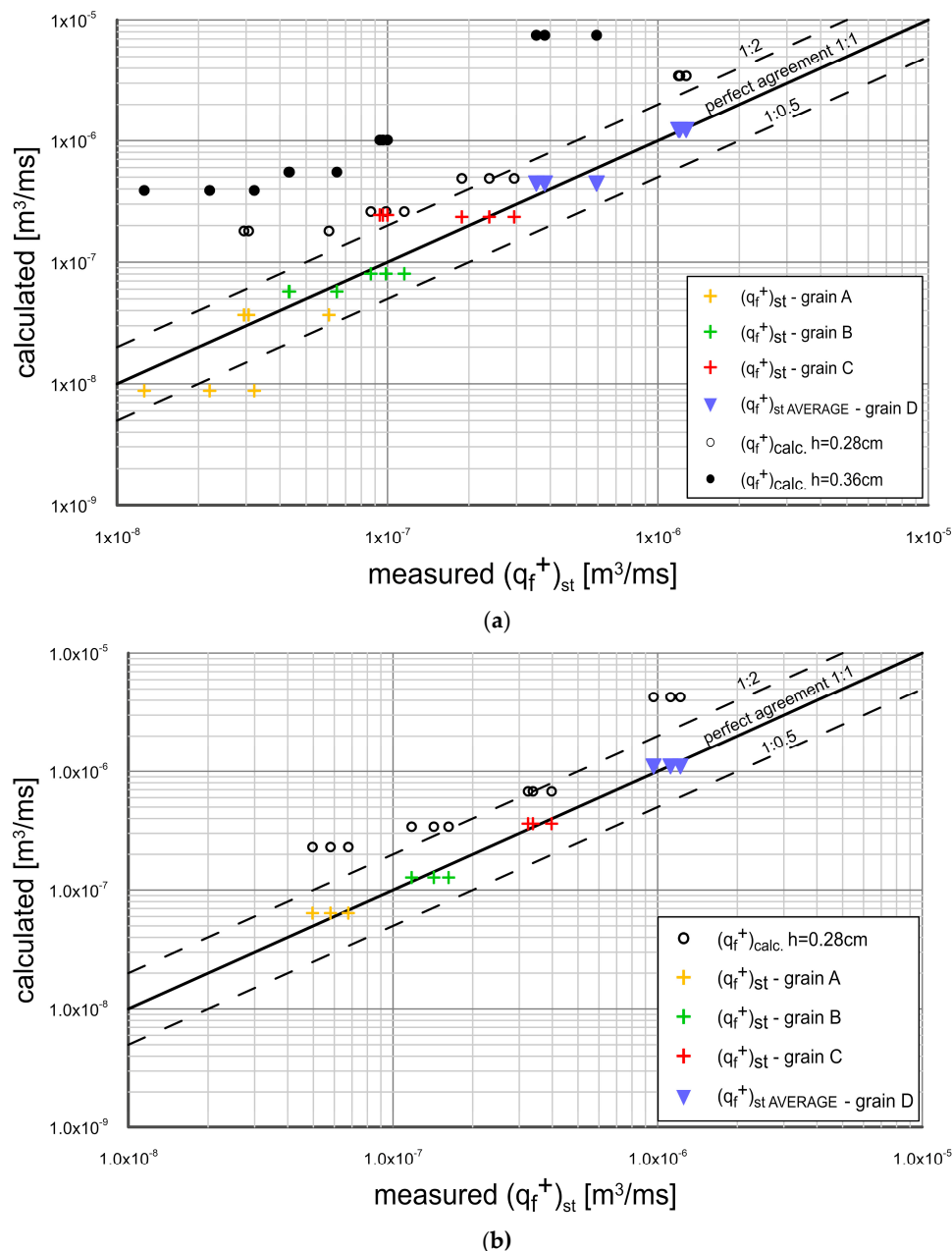


Figure 7. Comparison of calculation and measurements results q_f^+ between flat (a) and sloped bed (b) cases during the crest.

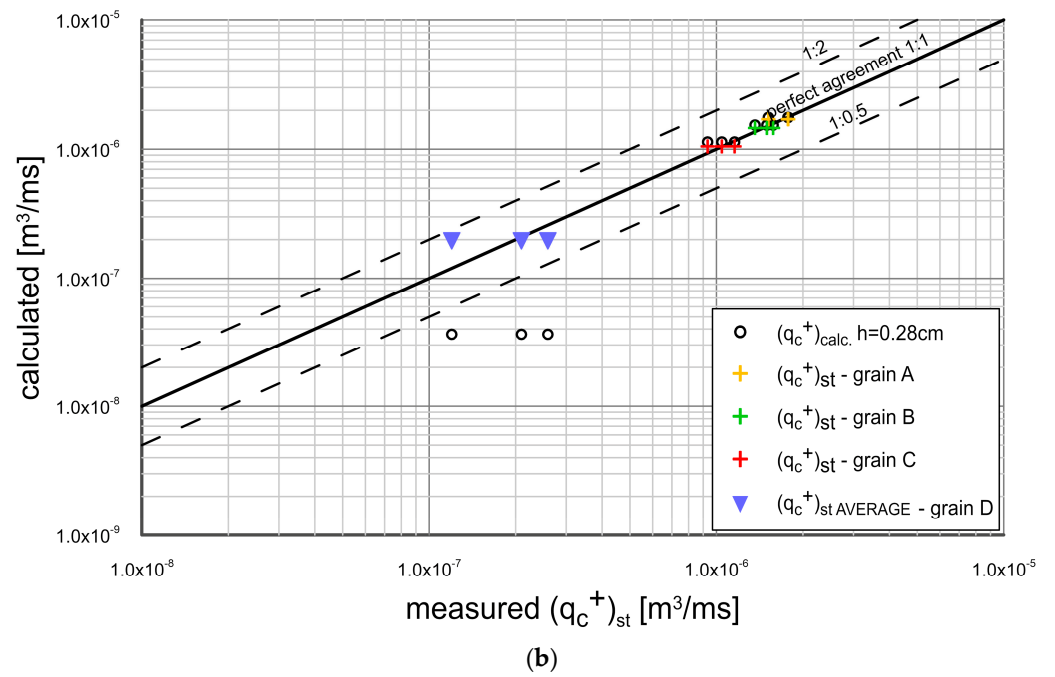
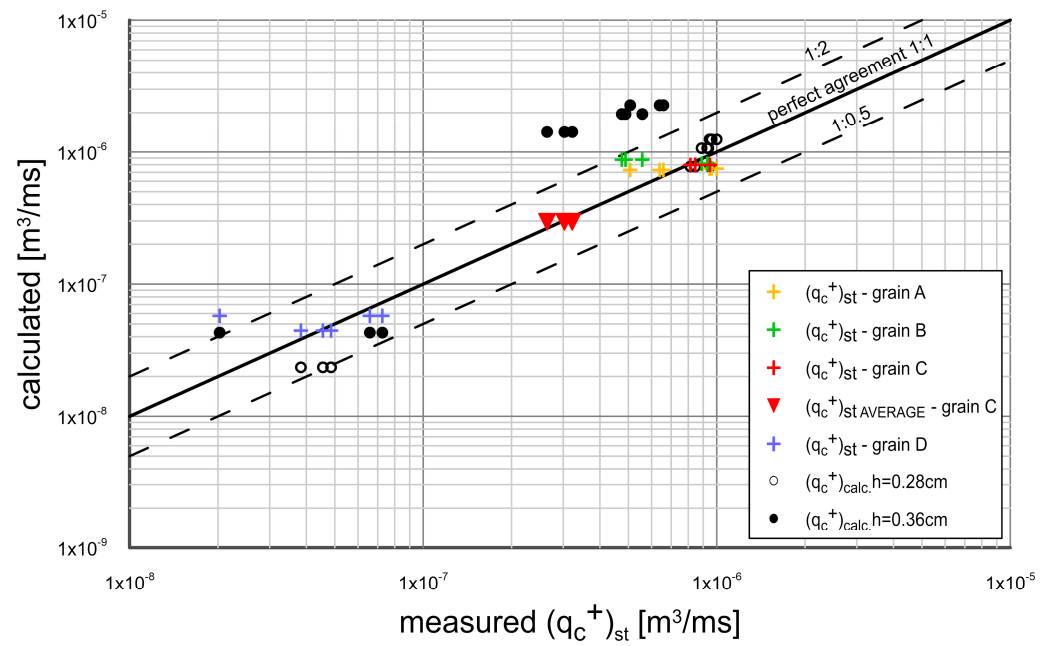


Figure 8. Comparison of calculation and measurements results q_c^+ between flat (a) and sloped bed (b) cases during the crest.

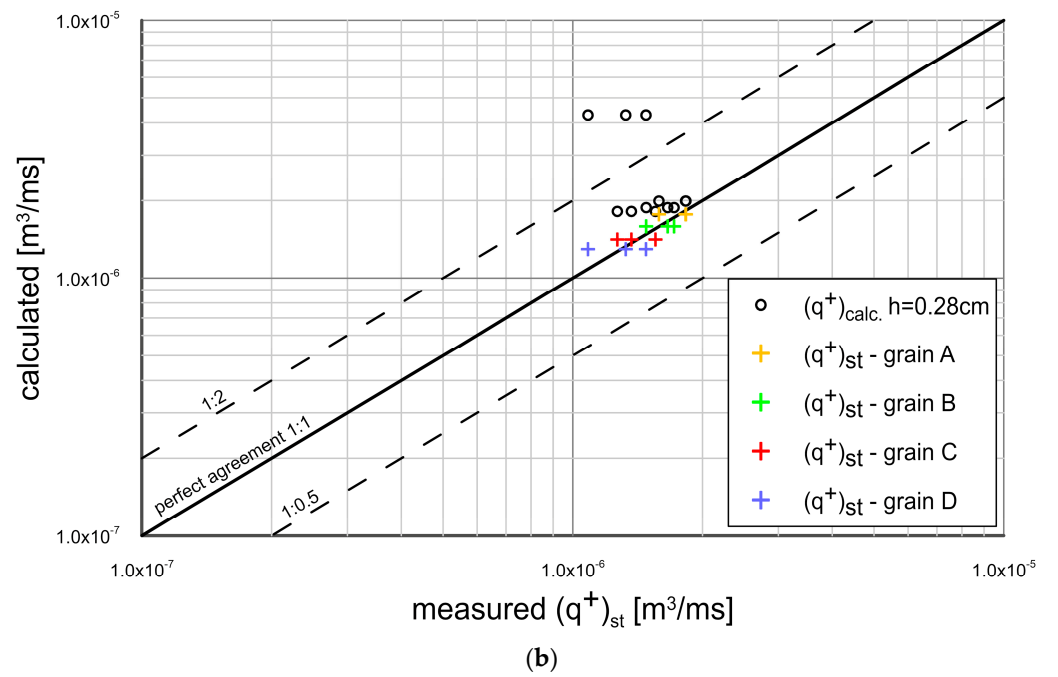
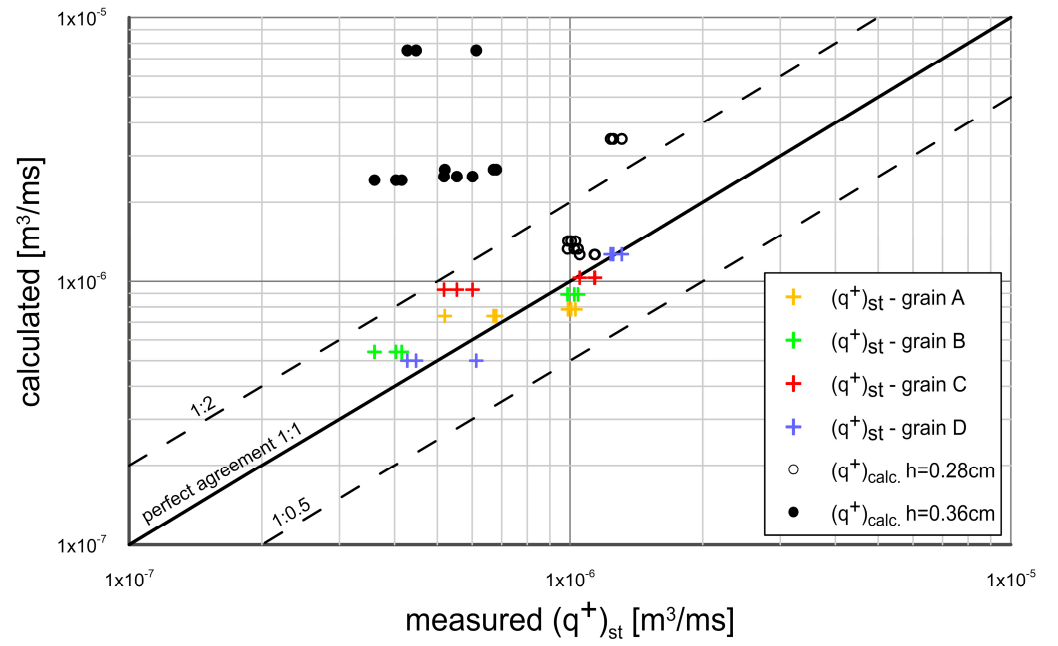


Figure 9. Comparison of calculation and measurements results q^+ between flat (a) and sloped bed (b) cases during the crest.

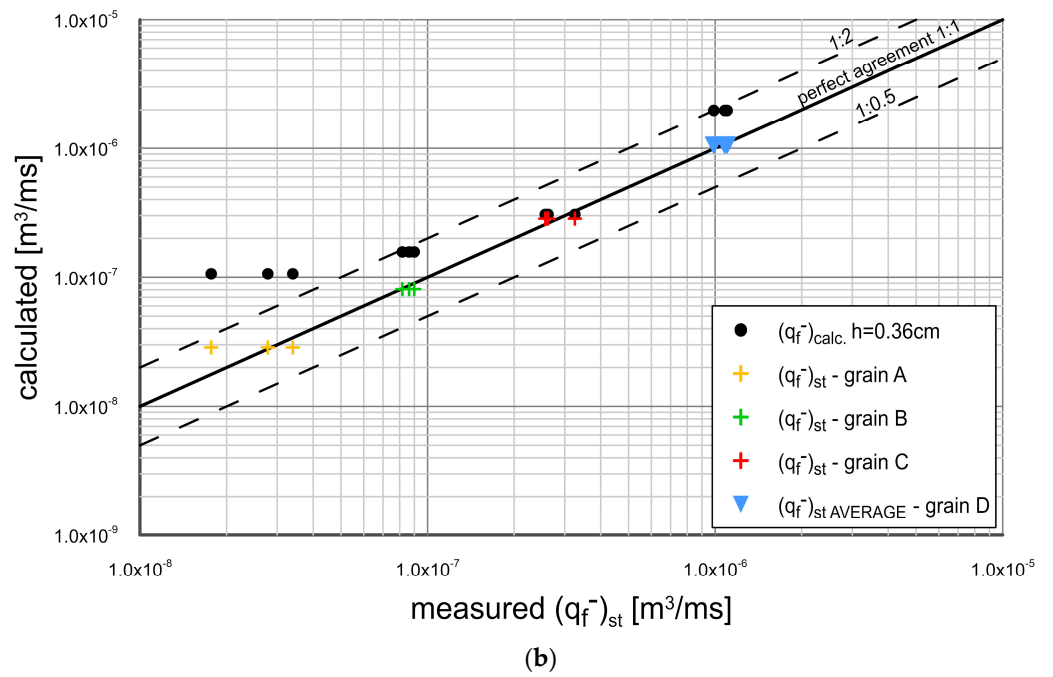
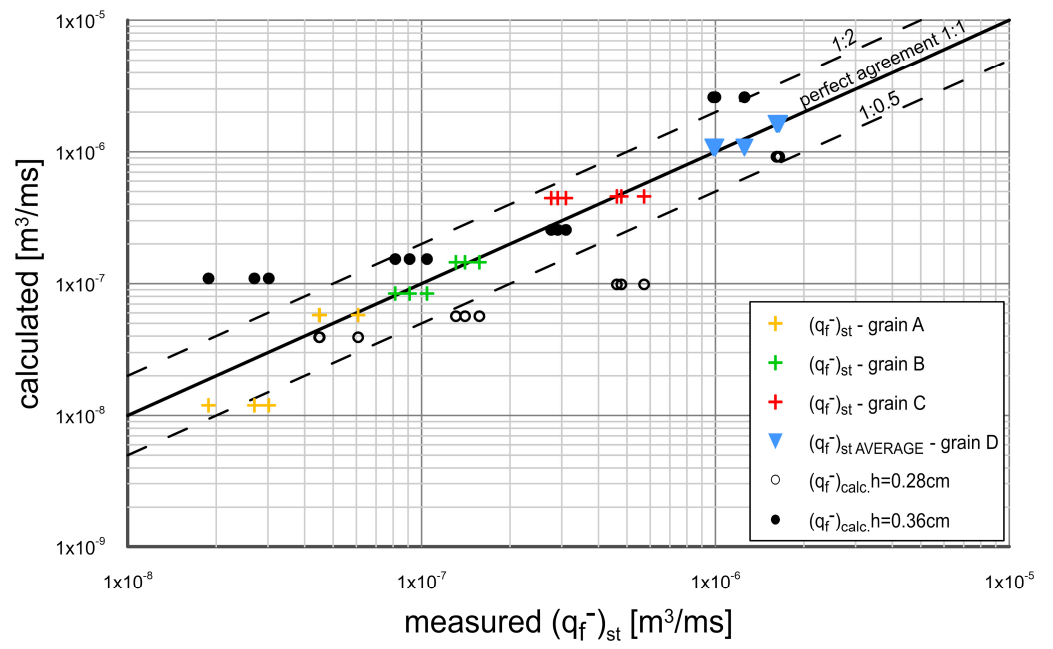
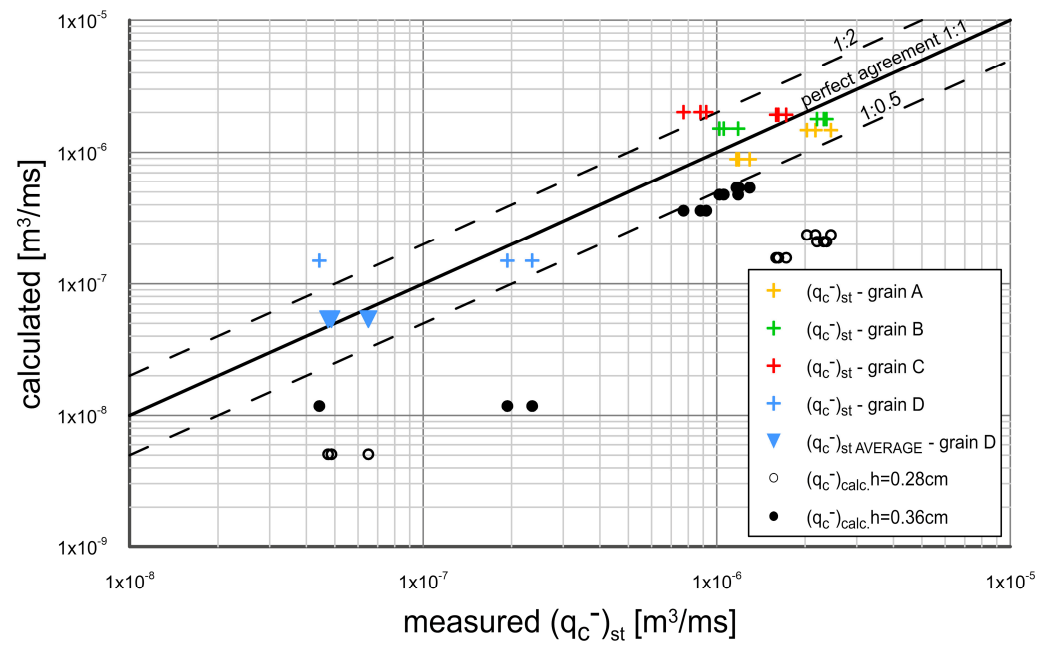
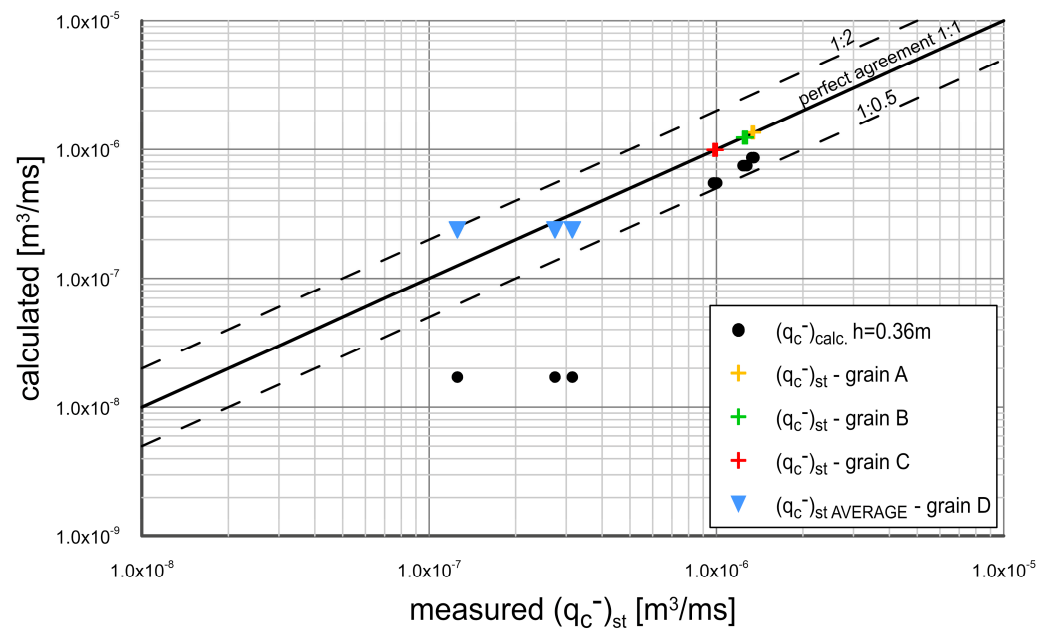


Figure 10. Comparison of calculation and measurements results \bar{q}_f^- between flat (a) and sloped bed (b) cases during the trough.



(a)



(b)

Figure 11. Comparison of calculation and measurements results q_c^- between flat (a) and sloped bed (b) cases during the trough.

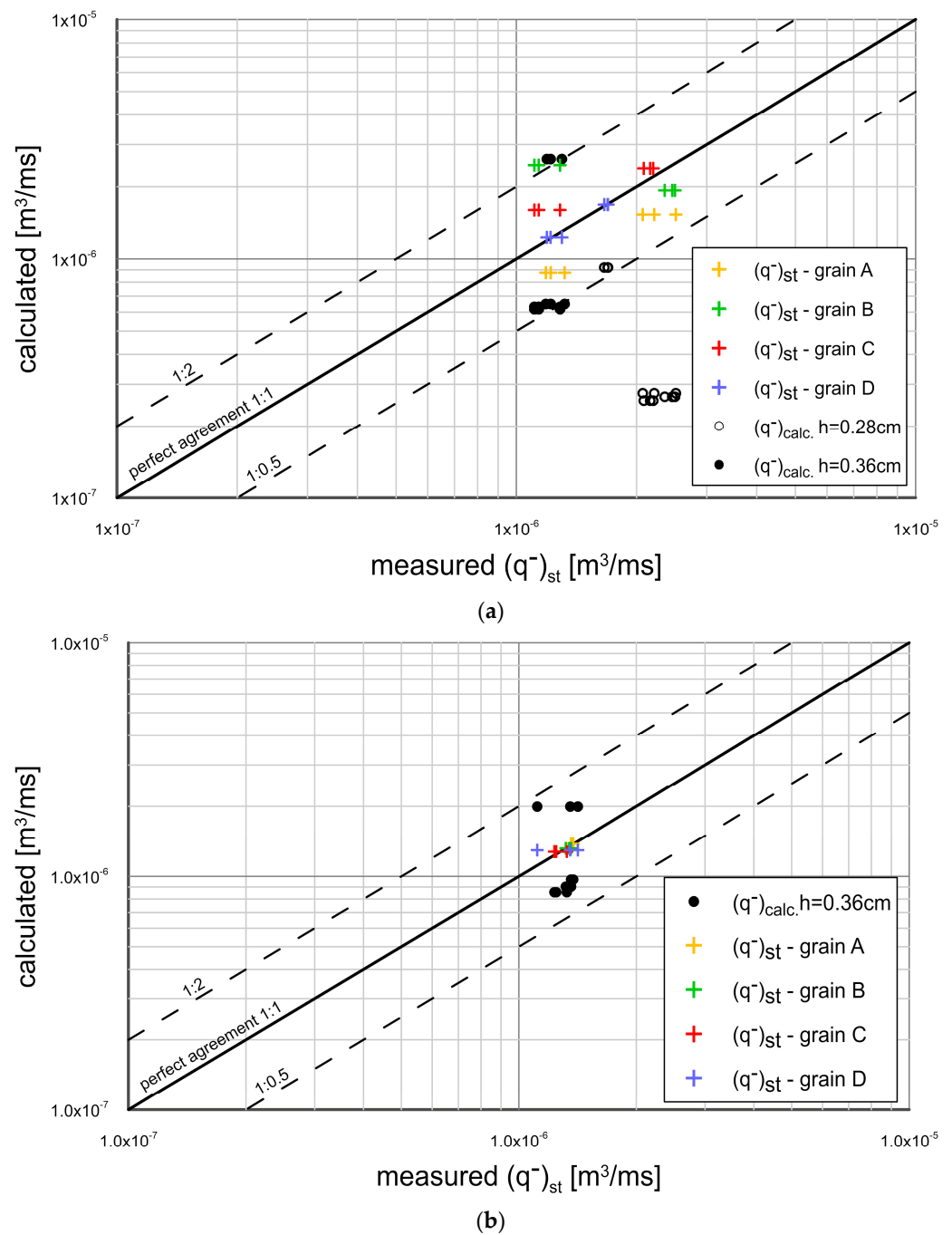


Figure 12. Comparison of calculation and measurements results q^- between flat (a) and sloped bed (b) cases during the trough.

3.5. Comparison of Grain Size Distributions Calculations with Measurement Results

Figure 13 shows a comparison of measured and calculated grain size distributions in the wave crest phase over the sloping bed for the four sands studied, with only a comparison of the calculated and measured total amount of fine and very fine fractions ($d_{50} < 0.20$ mm) for sand D with a large amount of fine and very fine fractions $n_f^{+/-} = \sum_{i=1}^{N_f} n_{fi}^{+/-}$ and the summed amount of coarse fractions $n_c^{+/-} = \sum_{i=N_f+1}^N n_{ci}^{+/-}$. The proportion of fine and very fine fractions $(n_f^{+/-})_{st}$ and coarse $(n_c^{+/-})_{st}$ was calculated by Formulas (16) and (17) for the crest phase and by Formulas (18) and (19) for the trough phase. Granulometric compositions were also calculated using the Kaczmarek et al. 2022 model, using Formulas (14) and (15).

The calculated granulometric compositions were compared with measurements of the granulometric compositions of sediments caught in trap A and B, respectively, in the trough and wave crest phases above the sloping bed. In addition, Figure 13 shows the measurement results of initial grain size distribution, with the proportion of fine and very fine fractions n_{fi} and coarse fractions n_{ci} sediments in the control area.

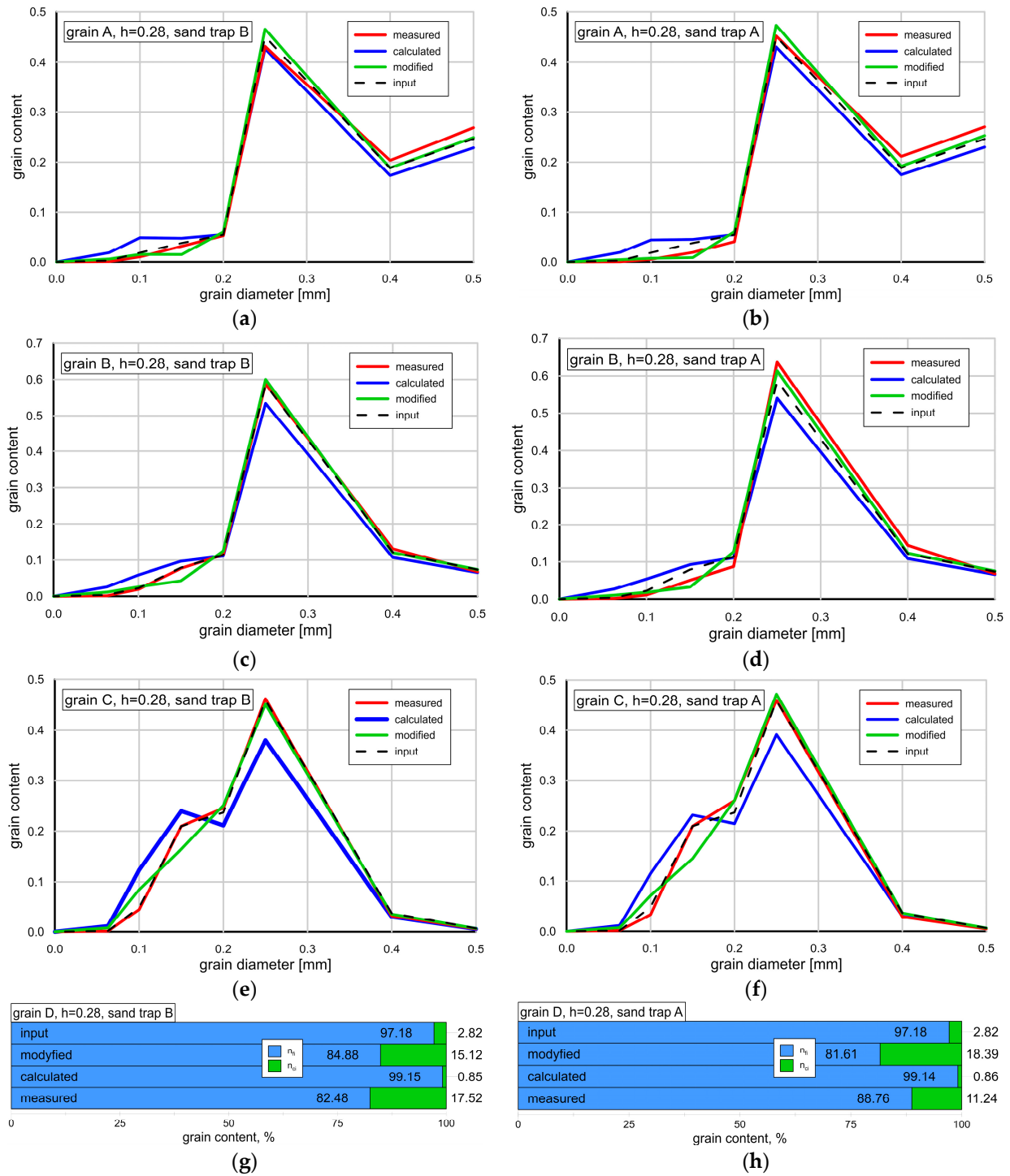


Figure 13. Comparison of calculated and measured grain size distributions in fine fractions and coarse fractions in sloped bed case: (a) sand A—crest; (b) sand A—trough; (c) sand B—crest; (d) sand B—trough; (e) sand C—crest; (f) sand C—trough; (g) sand D—crest; (h) sand D—trough.

It can be noted that in all cases the grain size distributions obtained with the three-layer model show an overestimation of the content of fine and very fine fractions ($d_i < 0.20$ mm) and an underestimation of the content of coarse fractions ($d_i \geq 0.20$ mm). This is due to the fact that the Kaczmarek et al. 2022 model does not take into account the effects of suspending the finest fractions in the higher layer above the bed and their return in the trough phase, and the effect of phase lags of fine fractions in the crest phase, and as a result, the incomplete flux of fine and very fine taken from the bed in the crest phase falls entirely into trap B (Figure 13a,c,e,g). In the trough phase, the Kaczmarek et al. 2022 model does not take into account the effect of finest fractions on the increase in content of coarse fractions (Figure 13b,d,f,h) falling into trap A. Therefore, it is worth emphasizing that the theoretical prediction with correction factors, resulting from the above effects for the sloping bed, gives values close to the measured ones.

Both in the crest phase (Figure 13a,c,e,g) in trap B and in the trough phase in trap A (Figure 4b,d,f,h), the proportion of fine and very fine fractions in sediments, measured and calculated with correction factors for all types of sand, is similar to the proportion measured in the input sediments. In turn, the proportion of these fractions, calculated with the Kaczmarek et al. 2022 model, shows significantly overestimated values. In contrast, the proportion of coarse fractions in both trap B and A, for all types of sands, calculated by the Kaczmarek et al. 2022 model provides significantly underestimated values relative to both the measured input distribution and the sizes measured in traps and calculated with correction factors.

4. Conclusions

Both theoretical and experimental analysis of sediment fluxes in the crest and trough of the wave outgoing from the control area over a sloping bed and comparison to the results over a flat bed allows the following conclusions to be drawn:

1. The vertical structure of total sediment transport with the content of very fine and fine ($d_i < 0.20$ mm) and coarse ($d_i \geq 0.20$ mm) fractions, both in the crest and trough of the wave, consists of components:
 - transport of outgoing sediment fluxes from the control area, which are deposited in adjacent control areas in both directions;
 - transport of fine and very fine sediment fluxes returning to the initial area in a suspended state;
2. Experimental results were compared with the results of theoretical analysis, based on the three-layer model of Kaczmarek et al. 2022. This model does not take into account the effects of additional vertical sorting of very fine sediment fractions and neglects the effects of phase lags of fine fractions, as well as does not take into account the effects related to the bed slope, i.e., effect of gravitational forces acting on grains, and the effect of pressure gradients when changing the flow cross section. Therefore, it was proposed to modify this model with the above-mentioned effects. Subsequently, calculations of the transport of fluxes of very fine and fine fractions, coarse fractions and total fractions outgoing in the crest and trough phases from the initial area and deposited in adjacent control areas were carried out and compared with the measurement results. The agreement of calculation results with measurements within \pm a factor two of the measurements was obtained. Calculations of granulometric distributions of sediments retained in adjacent areas from the crest and trough of the wave were also carried out. The calculated granulometric compositions were compared with the measurements and satisfactory agreement of the results was obtained for fine, very fine and coarse fractions;
3. Modification of the Kaczmarek et al. 2022 model was carried out based on four coefficients that correct the fluxes of fine and very fine fractions and coarse fractions that feed adjacent control areas on the crest and trough side of the wave. For sands with a relatively low content of fine fractions with $d_{50} \geq 0.20$ mm, it was possible to find a functional relationship of these coefficients with a determination coeffi-

cient $R^2 > 0.80$. For sands with a dominant amount of fine and very fine fractions ($d_{50} < 0.20$ mm), such a relationship could not be obtained, suggesting the need for further experimental research in this area.

4. Sediment transport over the sloping bed in the wave crest increases compared to the flat bed, due to the zone of negative pressure gradient. In the wave crest phase, due to higher hydrodynamic forcing, the fluxes deposited in the adjacent control area (falling into the trap) are larger than those in the flat bed situation. This results in better agreement between the results of calculations by the Kaczmarek et al. 2022 model and the results of measurements compared to those from a flat bed. This agreement deteriorates in case of sediments with a high content of fine and very fine grains, when the fluxes of coarse fractions falling into the trap and the fluxes of fine fractions returning to the initial area are increased;
5. In the trough, the situation is reversed—the intensity of sediment transport decreases due to the zone of positive pressure gradient. Due to lower hydrodynamic forcing, the outgoing fluxes toward the adjacent area, as well as the return fluxes in the wave crest are smaller than the fluxes in a flat bed situation. Virtually all of the outgoing flux feeds into the adjacent area (trap), and only a relatively small flux of the finest fractions returns in the wave crest to the initial area. This results in almost perfect agreement between calculations by the Kaczmarek et al. 2022 model and measurements. However, in case of sediment with a large number of fine and very fine fractions, their increased amount in suspension has a decisive influence on the transport of coarse fractions and finally results in an underestimation of the measured transport of coarse fractions by the Kaczmarek et al. 2022 model;
6. The influence of gravity forces reveals itself very strongly only in the trough phase when sediment is composed of coarse fractions and a small amount of fine and very fine fractions. However, in case of the greater amount of fine and very fine fractions in the bed, they have a decisive influence on the transport of coarse fractions in the trough phase, far exceeding the influence of gravity forces.

Author Contributions: Conceptualization, I.R. and L.M.K.; methodology, I.R., L.M.K., J.B., and M.P.; formal analysis, I.R., L.M.K., J.Z., J.B., M.P., and D.M.; investigation, I.R., L.M.K., J.Z., J.B., M.P., and D.M.; resources, L.M.K.; writing—original draft preparation, I.R., L.M.K., M.P., and D.M.; writing—review and editing, I.R. and L.M.K.; supervision, L.M.K.; project administration, I.R. and L.M.K.; funding acquisition, I.R. and L.M.K. All authors have read and agreed to the published version of the manuscript.

Funding: The research was financially supported by “ZINTEGROWANI—Kompleksowy Program Rozwoju Politechniki Koszalińskiej” nr POWR.03.05.00-00-Z055/18: Projekt współfinansowany ze środków Unii Europejskiej z Europejskiego Funduszu Społecznego w ramach Programu Operacyjnego Wiedza Edukacja Rozwój 2014–2020 and the research project of the Koszalin University of Technology, Faculty of Civil Engineering, Environmental and Geodetic Sciences: Dynamika niespoistego, niejednorodnego granulometrycznie ośrodka gruntowego w przepływie stacjonarnym i ruchu falowym w warunkach silnie nachylonego dna—funds no.: 524.01.07; project manager: L.K.

Data Availability Statement: The data presented in this study are available upon request from the corresponding author.

Conflicts of Interest: The authors declare no conflict of interest.

References

1. Wilson, K.C. Analysis of bed-load motion at high shear stress. *J. Hydraul. Eng.* **1987**, *115*, 825–830. [[CrossRef](#)]
2. Sumer, B.M.; Kozakiewicz, A.; Fredsøe, J.; Deigaard, R. Velocity and concentration profiles in sheet-flow layer of movable bed. *J. Hydraul. Eng.* **1996**, *11*, 549–558. [[CrossRef](#)]
3. Samaga, B.R.; Garde, R.J.; Ranga Raju, K.G. Total load transport of sediment mixtures. *Irrig. Power J.* **1985**, *42*, 345–353.
4. Karim, F. Bed material discharge prediction for nonuniform bed sediments. *J. Hydraul. Eng.* **1998**, *124*, 597–604. [[CrossRef](#)]
5. Wu, W.; Wang, S.S.Y.; Jia, Y. Nonuniform sediment transport in alluvial rivers. *J. Hydraul. Res.* **2000**, *38*, 427–434. [[CrossRef](#)]
6. Blom, A.; Ribberink, J.; Parker, G. Vertical sorting and the morphodynamics of bed form-dominated rivers: A sorting evolution model. *J. Geophys. Res.* **2008**, *113*, F01019. [[CrossRef](#)]

7. Khosravi, K.; Chegini, A.H.N.; Mao, L.; Rodriguez, J.F.; Saco, P.M.; Binns, A.D. Experimental Analysis of Incipient Motion for Uniform and Graded Sediments. *Water* **2021**, *13*, 1874. [\[CrossRef\]](#)
8. Sun, Z.; Zheng, H.; Xu, D.; Hu, C.; Zhang, C. Vertical concentration profile of nonuniform sediment. *Int. J. Sediment Res.* **2021**, *36*, 12–126. [\[CrossRef\]](#)
9. Ribberink, J.S. Bed-load transport for steady flows and unsteady oscillatory flows. *Coast. Eng.* **1998**, *34*, 59–82. [\[CrossRef\]](#)
10. Dohmen-Janssen, M.C. *Grain Size Influence on Sediment Transport in Oscillatory Flow*; Febodruk BV: Enschede, The Netherlands, 1999; ISBN 90-9012929-4.
11. Hassan, W.N. Transport of Size-Graded and Uniform Sediments under Oscillatory Sheet-Flow Conditions. Ph.D. Thesis, University of Twente, Enschede, The Netherlands, 2003.
12. Bailard, J.A. An energetics total load sediment transport model for a plane sloping beach. *J. Geophys. Res.* **1981**, *86*, 10938–10954. [\[CrossRef\]](#)
13. Shields, A. *Anwendung der Aehnlichkeitsmechanik und der Turbulenzforschung auf die Geschiebebewegung*; Erschienen im Eigenverlage der Preussischen Versuchsanstalt für Wasserbau und Schiffbau: Berlin, Germany, 1936.
14. Smart, G.M. Sediment transport formula for steep channels. *J. Hydraul. Eng.* **1984**, *110*, 267. [\[CrossRef\]](#)
15. Wong, M.; Parker, G. Reanalysis and correction of bed-load relation of Meyer-Peter and Müller using their own database. *J. Hydraul. Eng.* **2006**, *132*, 1159–1168. [\[CrossRef\]](#)
16. Damgaard, J.S.; Whitehouse, R.J.S.; Soulsby, R.L. Bed-load sediment transport on steep longitudinal slopes. *J. Hydraul. Eng.* **1997**, *123*, 1130–1138. [\[CrossRef\]](#)
17. Cheng, N.S.; Chen, X. Slope Correction for Calculation of Bedload Sediment Transport Rates in Steep Channels. *J. Hydraul. Eng.* **2014**, *140*, 843. [\[CrossRef\]](#)
18. Meyer-Peter, E.; Müller, R. Formulas for bed-load transport. In Proceedings of the 2nd Meeting of the International Association for Hydraulic Structures Research, Delft, The Netherlands, 7 June 1948; pp. 39–64.
19. Lamb, M.P.; Dietrich, W.E.; Venditti, J.G. Is the critical Shields stress for incipient sediment motion dependent on channel-bed slope? *J. Geophys. Res.* **2008**, *113*, F02008. [\[CrossRef\]](#)
20. Recking, A.; Frey, P.; Paquier, A.; Belleudy, P.; Champagne, J.Y. Bed-load transport flume experiments on steep slopes. *J. Hydraul. Eng.* **2008**, *134*, 9. [\[CrossRef\]](#)
21. Parker, C.; Clifford, N.J.; Thorne, C.R. Understanding the influence of slope on the threshold of coarse grain motion: Revisiting critical stream power. *Geomorphology* **2011**, *126*, 51–65. [\[CrossRef\]](#)
22. Maurin, R.; Chauchat, J.; Frey, P. Revisiting slope influence in turbulent bedload transport: Consequences for vertical flow structure and transport rate scaling. *J. Fluid Mech.* **2018**, *839*, 135–156. [\[CrossRef\]](#)
23. King, D.B. Studies in Oscillatory Flow Bedload Sediment Transport. Ph.D. Thesis, University of California, San Diego, CA, USA, 1991.
24. Tan, W.; Yuan, J. Modeling net sheet-flow sediment transport rate under skewed and asymmetric oscillatory flows over a sloping bed. *Coast. Eng.* **2018**, *136*, 65–80. [\[CrossRef\]](#)
25. Tan, W.; Yuan, J. Experimental study of sheet-flow sediment transport under nonlinear oscillatory flow over a sloping bed. *Coast. Eng.* **2019**, *147*, 1–11. [\[CrossRef\]](#)
26. Tan, W.; Yuan, J. Net sheet-flow sediment transport rate: Additivity of wave propagation and nonlinear waveshape effects. *Cont. Shelf Res.* **2020**, *240*, 104724. [\[CrossRef\]](#)
27. Box, W.; Järvelä, J.; Västilä, K. Flow resistance of floodplain vegetation mixtures for modelling river flows. *J. Hydrol.* **2021**, *601*, 126593. [\[CrossRef\]](#)
28. Khan, M.A.; Sharma, N.; Lama, G.F.C.; Hasan, M.; Garg, R.; Busico, G.; Alharbi, R.S. Three-Dimensional Hole Size (3DHS) Approach for Water Flow Turbulence Analysis over Emerging Sand Bars: Flume-Scale Experiments. *Water* **2022**, *14*, 1889. [\[CrossRef\]](#)
29. Lama, G.F.C.; Rillo Migliorini Giovannini, M.; Errico, A.; Mirzaei, S.; Padulano, R.; Chirico, G.B.; Preti, F. Hydraulic Efficiency of Green-Blue Flood Control Scenarios for Vegetated Rivers: 1D and 2D Unsteady Simulations. *Water* **2021**, *13*, 2620. [\[CrossRef\]](#)
30. Lama, G.F.C.; Errico, A.; Francalanci, S.; Solari, L.; Chirico, G.B.; Preti, F. Hydraulic Modeling of Field Experiments in a Drainage Channel Under Different Riparian Vegetation Scenarios. In *Innovative Biosystems Engineering for Sustainable Agriculture, Forestry and Food Production*; Coppola, A., Di Renzo, G., Altieri, G., D’Antonio, P., Eds.; Springer: Cham, Switzerland, 2020; pp. 69–77. [\[CrossRef\]](#)
31. Radosz, I.; Zawisza, J.; Biegowski, J.; Paprota, M.; Majewski, D.; Kaczmarek, L.M. An Experimental Study on Progressive and Reverse Fluxes of Sediments with Fine Fractions in Wave Motion. *Water* **2022**, *14*, 2397. [\[CrossRef\]](#)
32. Kaczmarek, L.M.; Biegowski, J.; Sobczak, Ł. Modeling of Sediment Transport with a Mobile Mixed-Sand Bed in Wave Motion. *J. Hydraul. Eng.* **2022**, *148*, 04021054. [\[CrossRef\]](#)
33. Kaczmarek, L.M. *Moveable Sea Bed Boundary Layer and Mechanics of Sediment Transport*; IBW PAN: Gdańsk, Poland, 1999; ISBN 83-85708-35-9.
34. Kaczmarek, L.M.; Ostrowski, R. Modelling intensive near-bed sand transport under wave-current flow versus laboratory and field data. *Coast. Eng.* **2002**, *45*, 1–18. [\[CrossRef\]](#)
35. Kaczmarek, L.M.; Biegowski, J.; Ostrowski, R. Modelling cross-shore intensive sand transport and changes of grain size distribution versus field data. *Coast. Eng.* **2004**, *51*, 501–529. [\[CrossRef\]](#)

36. Kaczmarek, L.M.; Sawczyński, S.; Biegowski, J. Hydrodynamic Equilibrium for Sediment Transport and Bed Response to Wave Motion. *Acta Geophys.* **2015**, *63*, 486–513. [[CrossRef](#)]
37. Kaczmarek, L.M.; Sawczyński, S.; Biegowski, J. An Equilibrium Transport Formula for Modeling Sedimentation of Dredged Channels. *Coast. Eng.* **2017**, *59*, 1750015-1–1750015-35. [[CrossRef](#)]
38. Kaczmarek, L.M.; Biegowski, J.; Sobczak, Ł. Modeling of Sediment Transport in Steady Flow over Mobile Granular Bed. *J. Hydraul. Eng.* **2019**, *145*, 04019009. [[CrossRef](#)]
39. Kaczmarek, L.M.; Radosz, I.; Zawisza, J. Numerical Calculations with a Multi-layer Model of Mixed Sand Transport Against Measurements in Wave Motion and Steady Flow. *Annu. Set Environ. Prot.* **2021**, *23*, 629–641. [[CrossRef](#)]
40. Malarkey, J.; Davies, A. Free-stream velocity descriptions under waves with skewness and asymmetry. *Coast. Eng.* **2012**, *68*, 78–95. [[CrossRef](#)]
41. Elfrink, B.; Hanes, D.M.; Ruessink, B.G. Parameterization and simulation of near bed orbital velocities under irregular waves in shallow water. *Coast. Eng.* **2006**, *53*, 915–927. [[CrossRef](#)]
42. Zou, Q.; Hay, A.E. The Vertical Structure of the Wave Bottom Boundary Layer over a Sloping Bed: Theory and Field Measurements. *J. Phys. Oceanogr.* **2003**, *33*, 1380–1400. [[CrossRef](#)]

Disclaimer/Publisher’s Note: The statements, opinions and data contained in all publications are solely those of the individual author(s) and contributor(s) and not of MDPI and/or the editor(s). MDPI and/or the editor(s) disclaim responsibility for any injury to people or property resulting from any ideas, methods, instructions or products referred to in the content.